CHALMERS

Fast refueling of Volvo hydrogen trucks

Bachelor's thesis in Automotive Engineering

Oskar Forsström

Johan Loebbert

DEPARTMENT OF MECHANICS AND MARITIME SCIENCES

Chalmers University of Technology
Gothenburg, Sweden 2023
www.chalmers.se

BACHELOR'S THESIS 2023

FAST FUELING OF VOLVO HYDROGEN TRUCKS

OSKAR FORSSTRÖM, JOHAN LOEBBERT

CHALMERS

DEPARTMENT OF MECHANICS AND MARITIME SCIENCES

CHALMERS UNIVERSITY OF TECHNOLOGY
GOTHENBURG, SWEDEN 2023

SUPERVISOR: PER HANARP (VOLVO) – PRINCIPAL ENGINEER HYDROGEN INFRASTRUCTURE TECHNOLOGIES

EXAMINER: MATS ANDERSSON (CHALMERS) – DOCENT AT ENERGY CONVERSION AND PROPULSION SYSTEMS

Abstract

Volvo is currently investigating fuel cell electric vehicles and using hydrogen as fuel. The fuel cell trucks carry high pressure hydrogen storage systems with carbon fiber reinforced polymer tanks. Fueling of hydrogen in a fast and safe manner is a topic under investigation. The aim for Volvo is to perform a fueling process in less than 10 minutes using new or existing protocols, staying within tank design limits when it comes to end pressure and temperature in the tank. In this report, Volvo's prototype truck, A1, was studied during refueling in a simulation environment using the software H2FillS. Parameters, such as ambient temperature, pre-cooling and gas temperature were varied. H2FillS results were compared to a field test and another modeling software, GT-Suite, with the same input conditions. The results unveiled that ambient temperature has a minor influence on the gas end temperature in the tanks after refueling is done, whereas the initial gas temperature within the tanks has a major influence. Most impact has pre-cooling temperature of the hydrogen before it is dispensed into the vehicle, and a temperature of at least -20 °C is essential for refueling to be performed within the time goal. Finally, different protocols were applied, and it was shown that fueling in 10 minutes can be done under most conditions.

Acknowledgement

The work behind this report could not have been made without our supervisor, Per Hanarp. Therefore, we would like to thank him for his patience, guidance, valuable insights, but most importantly, his genuine interest in our project.

We would also like to thank Aishwarya Nair and Anton Hagby for their input, assistance, and guidance in this thesis as well as our examiner, Mats Andersson.

List of Acronyms

Below is a list of acronyms used in the report, listed in alphabetic order:

$APPR$	Average pressure ramp rate
BEV	Battery electric vehicle
CCH_2	Cryo-compressed hydrogen
$CFRP$	Carbon fiber reinforced polymer
CGH_2	Compressed gaseous hydrogen
$CHSS$	Compressed hydrogen storage system
CO	Carbon monoxide
CO_2	Carbon dioxide
FC	Fuel cell
$FCEV$	Fuel cell electric vehicle
H_2	Hydrogen
$HDEV$	Heavy duty electric vehicle
H_2O	Water
HSS	Hydrogen storage system
He	Helium
ICE	Internal combustion engine
MTJ	Multi-tank junction
NO_x	Nitrogen oxide
O_2	Oxygen
OEM	Original equipment manufacturer
OTV	On tank valve
PEM	Polymer electrolyte membrane
PRR	Pressure ramp rate
SOC	State of charge

Contents

List of figures

1.Introduction

1.1 Background

The world as we know it is facing a significant threat on climate change. Due to release of greenhouse gases into the atmosphere over many years, particularly carbon dioxide (CO_2), the average temperature on Earth rises. That causes an increased frequency of extreme weather events, as well as long term risks for water scarcity, loss of agricultural lands, raising sea levels et cetera. The total amount of direct CO_2 emissions globally 2022 reached 36,8 Gt (gigatons) where the transportation sector was responsible for 7,98 Gt, or 21,7% of the emissions [1].

The Paris agreement sets the international framework to minimize the emission of climate gases and keep global warming at well below 2 °C. Climate targets also heavily affect the automotive industry with stricter regulations on CO_2 emissions. The transportation sector is currently going through a transition from fossil to renewable energy with a variety of alternative solutions to substitute burning fossil fuel in conventional internal combustion engines (ICEs). One energy carrier being investigated is using hydrogen (H_2) to power a fuel cell (FC), turning the gas into electricity in a fuel cell electric vehicle (FCEV).

Today, most of Volvo's truck fleet uses an ICE but the company is heavily investing in new "zero emission" technologies. One part is the fuel cell electric vehicles, alongside battery electric vehicles (BEV) and internal combustion engine vehicles running on renewable fuels.

Battery electric trucks are currently launched by many suppliers including Volvo and are appropriate for many applications. However, for most long range and demanding applications the amount of stored energy in batteries may not be enough. Another drawback is charging times and temperature sensitivity. Recharging a large battery pack takes significantly longer than refueling a vehicle with conventional fuel. Batteries temporarily lose capacity if temperature falls below freezing temperatures which also can cause the batteries to degrade faster over time, especially if also frequently charged rapidly, which in itself degrades a battery. On the other hand, a BEV is a relatively simple system, fundamentally consisting of only an electric motor(s) and a battery pack, which may require less service.

A fuel cell electric vehicle is a relatively complex system consisting of a fuel cell, batteries, a hydrogen storage system, a cooling system, and an electric motor. The fuel cell could be considered a small power plant using hydrogen to produce electricity used by the electric motors or stored in small batteries as an energy buffer. This process only emits heat and water (H_2O) without the harmful emissions nitrogen oxide (NO_x), carbon monoxide (CO) or CO_2. The FCEV needs batteries too but only as an energy buffer for power transients, while the main energy is stored in the gas. Battery degradation is applicable here just as in the BEV.

Additionally, the fuel cell also degrades over time depending on operating conditions. The most prominent degradation occurring in a polymer electrolyte membrane (PEM) fuel cell is the catalyst layer being damaged due to carbon corrosion. Area in the catalyst is also successively lost due to platinum dissolution and sintering due to voltage cycling. The degradation phenomenon cannot be completely suppressed but minimized by optimizing operating conditions for the fuel cell to work as close to an ideal work cycle as possible. Apart from the factors mentioned above, there are other chemical, thermal and mechanical ways of

degradation affecting the fuel cell, factors such as vibrations and shock, particles in the air, temperature conditions and gaseous contamination. [3]

FCEVs and BEVs are electric vehicles using electric motors for propulsion and can both be considered emission contributors/free depending on where the electricity or hydrogen is produced for the BEV and FCEV, respectively. Both solutions have benefits and limitations where one system may be preferable in one situation rather than the other.

A challenge with using hydrogen is storing it in a practical and safe way, this report considers storing the gas in a compressed hydrogen storage system (CHSS). Although hydrogen is quicker to refuel than to charge a battery pack of equivalent energy capacity, it requires steeper safety measures to be executed in a safe manner. This is due to the properties of H_2, which is stored at a very high pressure of 700 bar (70MPa), in carbon fiber reinforced polymer tanks. The tanks have design limits when it comes to pressure and temperature and a fueling protocol is needed not to damage the tanks and to stay within safe limits. This work investigates impacts on different initial conditions for temperature and pressure on the fueling process and end state in the tanks. In addition, new types of fueling protocols applied to Volvo Truck prototype vehicle design are evaluated.

1.2 Aim (scope)

The aim for this thesis is to perform simulations in a H_2 refueling simulation software, H2FillS, to understand how the refueling time is affected by factors such as ambient temperature, tank temperature and pressure et cetera. The Volvo fuel cell A1 truck design is implemented in the simulation software. The results will be compiled and evaluated with respect to safety, refueling time and temperature/pressure boundaries in different refueling protocols.

As well as the evaluation above, the data from H2FillS will also be compared with another simulation software, GT-SUITE, and with field-test data.

1.3 Limitations

Hydrogen refueling is a subject too large to cover in this report, therefore, limitations are set. Below is a list of subjects that are not considered in this report.

- Cryo-Compressed Hydrogen (CCH_2).
- Liquid Hydrogen (LH_2).
- Production of H_2
- Stationary CHSS. That is the CHSS stationary at refueling stations providing H_2 for vehicles.
- The fuel cell's function in detail.
- Temperature differences inside CHSS (thermal stratification).

1.4 Problem and specific aim

The target is for a truck to refill the vehicle's H_2-tanks as quickly as possible without compromising operator, system, or material safety marginals. Volvo's tanks can carry a total of 37 kg hydrogen in its compressed gaseous state. Ideally the refueling performance should be similar or better than today's standard procedure for conventional gas and diesel trucks.

The set conditions are:

Refueling time	≈ 10 minutes
Maximum allowed tank pressure	875 bar at 85 °C
Maximum nominal tank pressure	700 bar at 15 °C
Max fuel capacity	37 kg (185 *5 L)
Maximum degree of filling	100%
Allowed temperature interval	-40 to +85 °C

The refueling time can be controlled by increasing or decreasing the pressure ramp rate from the hydrogen fuel station.

2 Theory

2.1 Hydrogen

H_2 is the lightest and most abundant element in the universe and the main constituent of stars. On Earth it is mostly bound in other elements and rarely found pure, only 0.000055% (0.55 ppm) of the atmosphere contains its pure form [4]. The gas is not toxic, has no color, smell or taste and is easily combustible.

Comparing the energy density of H_2 in its gaseous state, compressed to 70 MPa (700 bar) and at a temperature of 15 °C, to conventional diesel in a liquid state, H_2 has a mass density of 0,084 kg/m^3 (at atmospheric pressure) and an energy density of 4,8 MJ/L, compared to diesel (B0) with a mass density of 832,0 kg/m^3 and 35,8 MJ/L respectively. H_2 has a higher heating value of 120 MJ/kg compared to diesel with 43,1 MJ/kg. The drawback is that H_2 in a gaseous state takes up a lot more volume to achieve the same mass [5].

H_2 can be used in a liquid as well as a gaseous state, and in a cryogenic-compressed state which is a compressed form cooled just above condensation temperature. Holding it in a fully liquid state at atmospheric pressure increases the energy density (MJ/L) significantly but requires an advanced and energy consuming procedure whereas the H_2 must be cooled down and kept at a temperature of around 20 K, or -253 °C [6]. Figure 1 below illustrates the properties and behavior of hydrogen under different pressure and temperature.

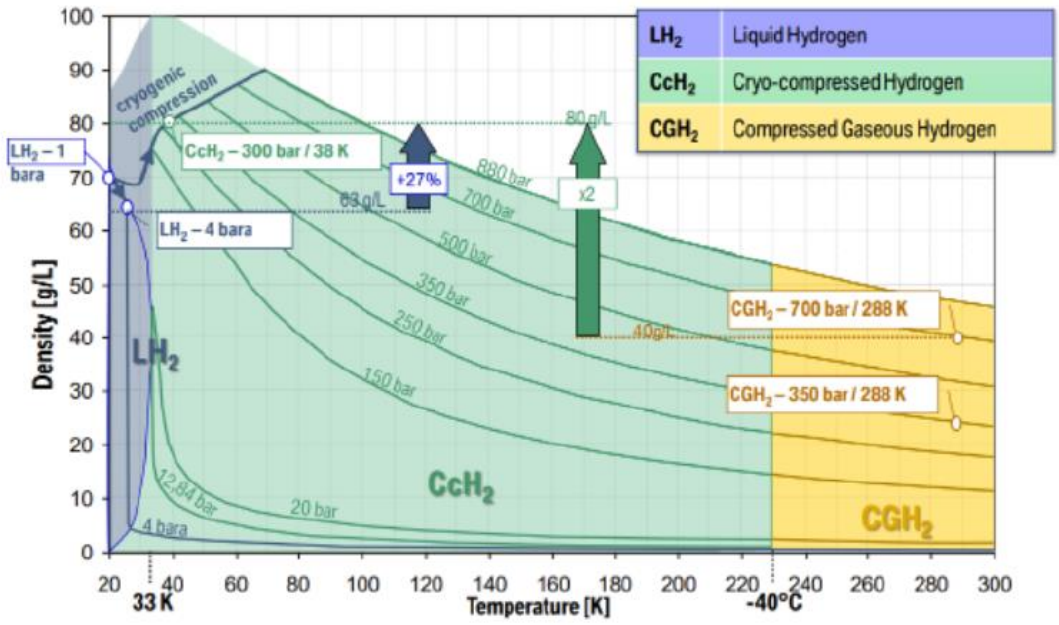

Fig. 1. Phase diagram of hydrogen. From [7]

2.2 Heating of gas during fueling

The main concern during refueling of compressed hydrogen is the heating of the gas that occurs. This has two reasons, heating of compression and the reverse Joule-Thomson effect [8].

2.2.1 Heating of compression

During refueling the gas is compressed in the vehicle tank. According to the ideal gas law $pV = nRT$, which indicates that with constant volume (V), molar mass (n) and gas constant (R) the temperature rises with increased pressure and vice versa.

2.2.2 Joule-Thomson effect

The other of the main concerns is the thermodynamic phenomenon called the 'Joule-Thompson effect'. It describes the temperature change in a process of a gas (fluid) expanding from a higher to a lower pressure with the internal kinetic energy remaining mostly constant. Generally, gases cool down at room temperature and atmospheric pressure when exposed for such expansion, except for helium (He) and H_2. These gases have properties that instead causes them to increase in temperature during the same process. In this context it means the H_2 in the CHSS heats up during refueling due to the rapid gas expansion from the pipes to the storage tanks where a significant pressure difference is prominent. This is highly relevant to take into consideration when designing and configuring the refueling process [9] [10].

2.3 Storage tanks

Hydrogen storage tanks are typically cylinders of metal or composite coated with an inner liner to protect the tanks from hydrogen embrittlement. The tanks are currently classified in four standards where each have different advantages depending on the objective of the CHSS. The four different types are as follows [11]:

- Type I. All-metal cylinder, most commonly steel, resulting in a heavy product and therefore often used as stationary storage with the ability to withstand a pressure of 200-300 bar.
- Type II. Full metal cylinder wrapped with composite.
- Type III. Full composite cylinder with an inner liner of aluminum acting as a barrier to eliminate any risk of embrittlement. Designed to withstand 450 bar.
- Type IV. Full composite of carbon fiber in an epoxy matrix with an inner liner made of plastic. Maximum pressure up to 1000 bar.

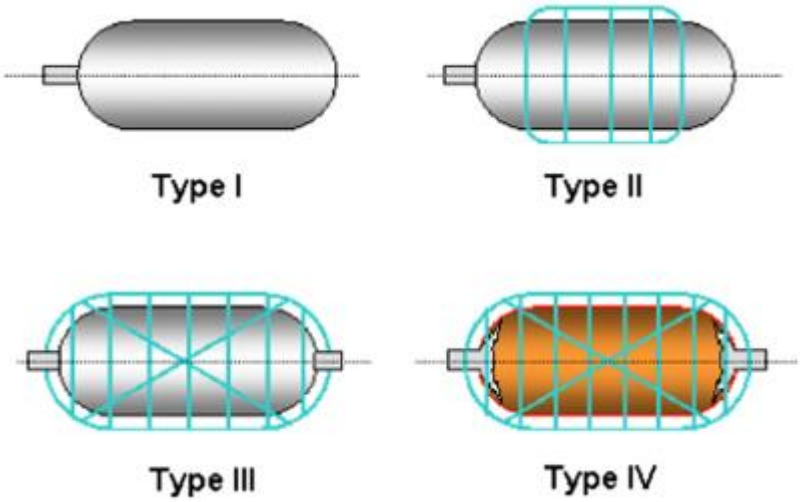

Fig. 2. Hydrogen storage tanks schematic. From [12]

Figure 2 above illustrates the different types of a storage tank. Due to light weight and high-pressure resistance Type III and IV are more suitable for the automotive industry, however,

they are more expensive [11]. Neither Type 1 or II are suitable for automotive industry due to weight and risk of embrittlement.

2.4 Fuel cell

The basic principle of the FC is to convert H_2 into electricity through a redox reaction (reduction-oxidation) and it acts like a small power plant producing electricity with H_2O and heat as by-product [13]. Fig. 3. schematic illustrates the reactant steps of H_2 and O_2 to H_2O and electricity in a FC.

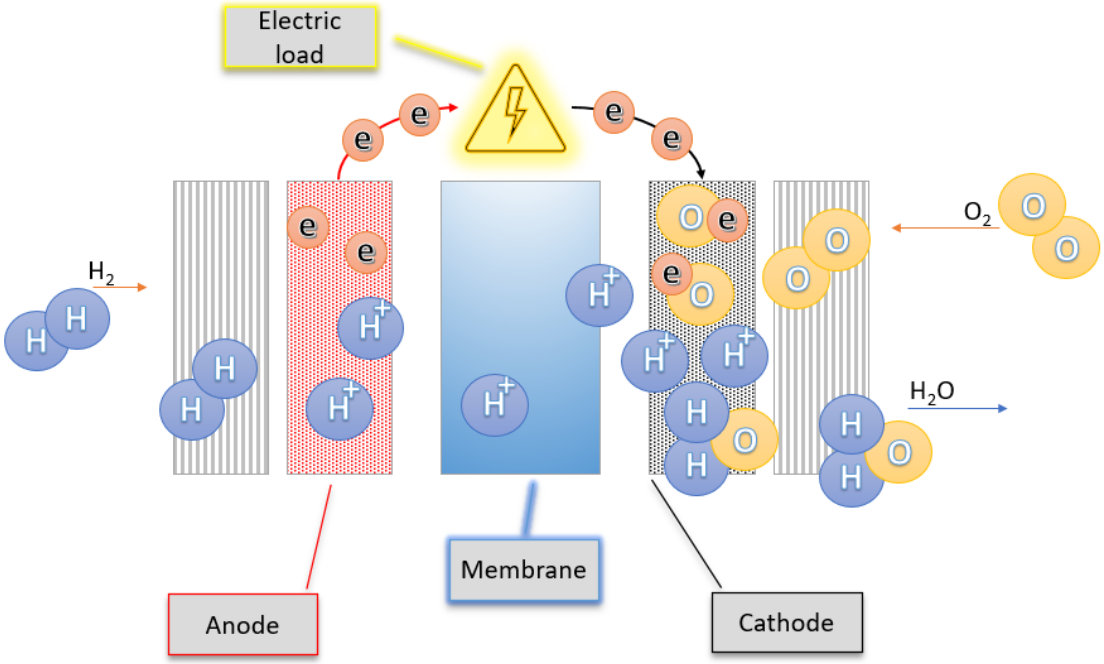

Fig. 3. Fuel cell schematic.

The fundamental principle of the chemical process is that H_2 enters via the anode in the FC where the proton (H^+) and electron (e) are separated. The proton can pass through the carbon membrane to the cathode, but the electrons cannot. This results in an electrical potential in the FC to which you can connect a load, in this case an electric motor. The electricity (electrons) can flow through this load and the potential creates an electrical current. When the electrons and protons reach the anode, they react with the oxygen (O_2) in the air, creating tailpipe emissions consisting of H_2O and heat. [14]

2.5 Batteries

A FC works most efficiently and lives the longest when working under a moderate and consistent load. Sudden transients in power output will damage the components in the long term and reduce its efficiency, that is where batteries come in. Batteries work as a buffer and are used in hybridization mode with the FC due to their ability to deliver a lot of instantaneous power. When lots of sudden energy is needed, for example when accelerating quickly uphill, the excess electricity generated by the FC stored in the batteries will be used to power the motors. This allows the FC to keep working at a relatively constant pace [15]. Also, batteries degrade with transient operations therefore a suitable power split control strategy is needed for optimal lifetime of the whole system.

2.6 Refueling- Station and Process

The refueling station transfer hydrogen from one high pressure storage to another. At the station dispenser outlet, the H_2 is cooled down to subzero degrees Celsius to in some way reduce the heating effects described in section 2.2 before being transferred to the vehicle [16]. This is often referred to as pre-cooling.

It is important to consider the final pressure and temperature when refueling a CHSS. These two parameters have an upper limit that must not be exceeded. A 700-bar nominal pressure tank has an operating limit of +85 °C at 875 bar. Simultaneously, the target is to reach 100 percent at state of charge (SOC). That means there is a specific operating window when refueling. Figure 4 below demonstrates, in a simplified but effective way, the fueling window where the SOC at 100% can be tracked with respect to pressure and temperature for a tank with 700 bar as nominal working pressure.

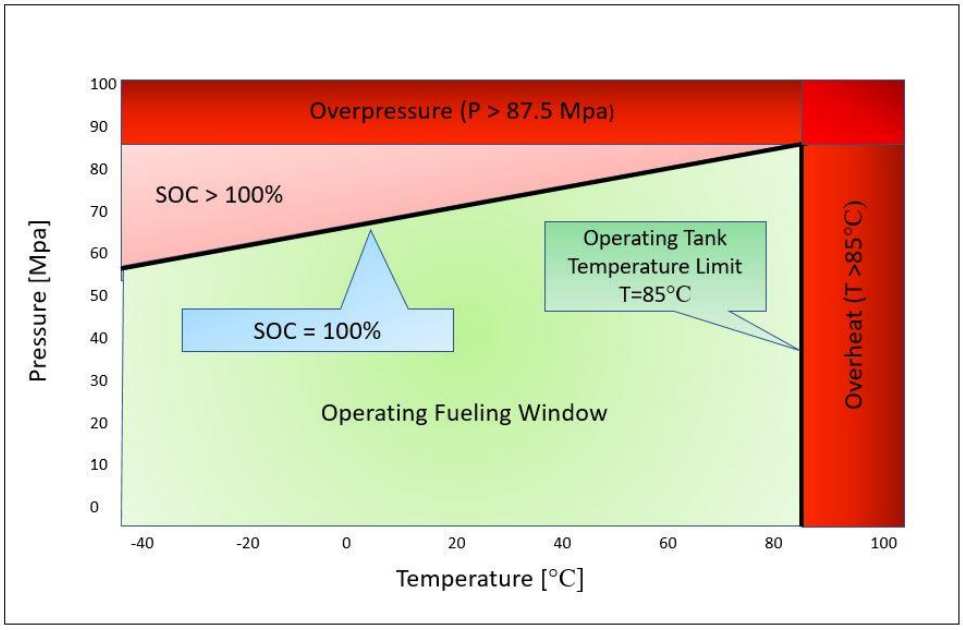

Fig. 4. Fueling Window.

The black line, where SOC is at 100%, is the roof of how much hydrogen can be stored at a specific temperature and pressure. As the chart states, different final temperature values (T_{final}) has a different maximum pressure (P_{max}) with SOC at 100% as a terminating condition for the refueling.

2.6.1 Average Pressure Ramp Rate (APRR)

The APRR (MPa/min) is a linear ramp calculated by the fuel station to reach 100% SOC within the operating fueling window. When a vehicle is connected to refuel, the station dispenses a pressure spike, also known as the connection pulse, to estimate the initial tank pressure (P_{init}). Collectively with initial parameters as ambient temperature (T_{amb}) and fuel delivery temperature the APRR is set. The process of the APRR is illustrated in figure 5 below.

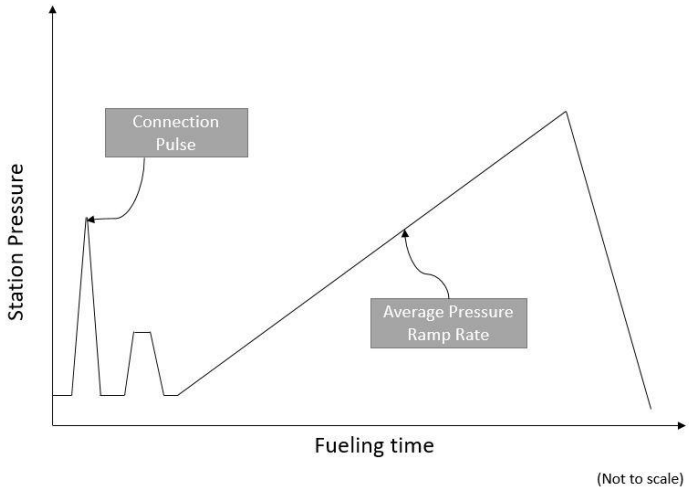

Fig. 5. Hydrogen Pressure Development and APRR (at station).

The figure above demonstrates the pressure spike and how the pressure during a refueling process increases with time. The station receives a response-pressure from the CHSS and then the APRR is set. The steep slope in the end is the station depressurizing the refueling system.

2.6.2 PHRYDE – Protocol for Heavy-Duty Hydrogen Refueling

Project PHRYDE was established in 2020 and was based on fueling protocols already existing to develop several new protocol concepts for fueling of larger vehicle based CHSSs utilizing systems with 35, 50 and 70 MPa as nominal working pressure [17]. Through calculations, simulations and almost three years of work project PHRYDE ended and left behind valuable information and guidance regarding hydrogen infrastructure.

A protocol is what the fueling station uses to calculate the pressure ramp rate (PRR) that should be used. There are different varieties of protocols that uses different input information to optimize the refueling process [18]. The input data depend on the incoming vehicle's communication level (one way or two way). The fueling station provide the ambient temperature (T_{amb}) and fuel delivery temperature (T_{fuel}). The vehicle may transmit extra information such as static and dynamic data related to tank pressure, temperature and system configuration [18]. The biggest factor affected by which protocol is used is the total refueling time.

The protocol uses a set of input parameters to set an optimal PRR to fuel as fast as possible without going outside the safe fueling window as described in figure 2. Input data can be:

- Ambient temperature
- Tank pressure (identified by station through a sensor in the vehicle tank)
- Tank temperature
- Tank size(s), geometry, and material properties

With no or limited input data the PRR is set conservative and gives long fueling times. With more input data, the PRR can be set higher and reduces fueling time and still operate within the safe window, see figure 6. The PRR is calculated based on thermodynamic simulations (as H2FillS software) and experimental knowledge and is presented as tables based on ambient temperature and station pre-cooling (see below). It is important that sensor measurements can be trusted, and redundancy may be needed for certain measurements to ensure safety.

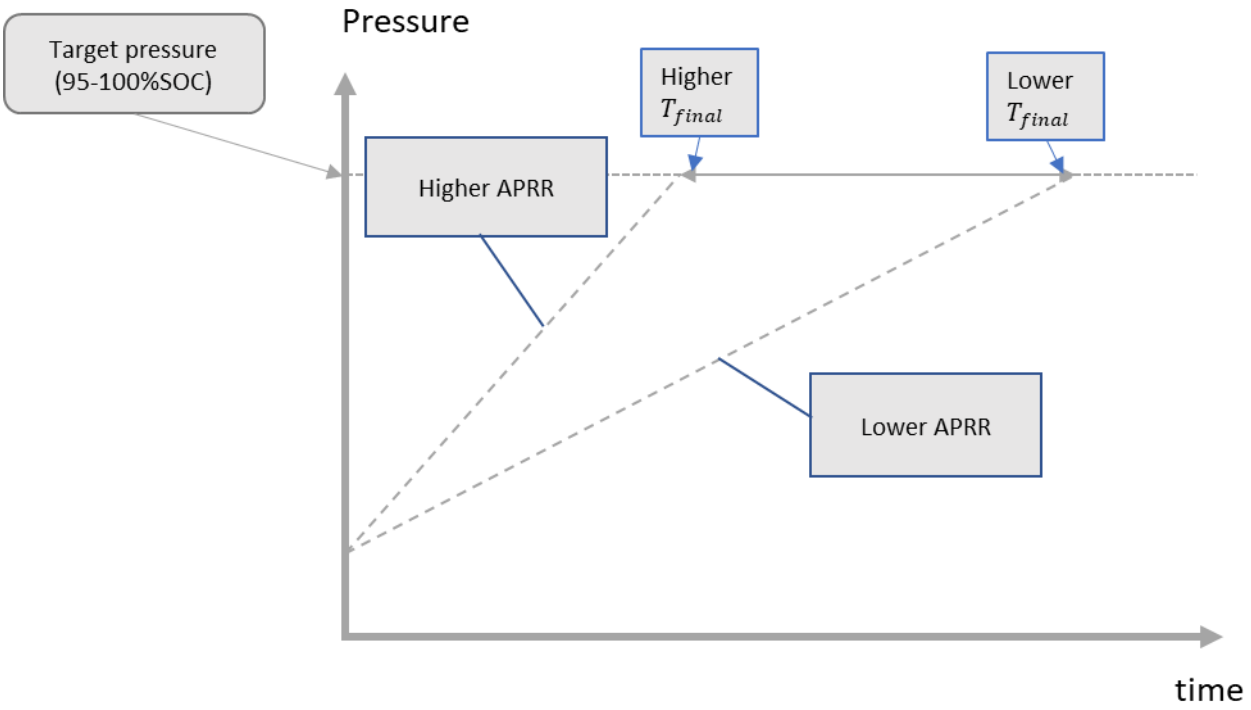

Fig. 6. Safe and fast refueling

From the chart above it is obvious that higher APRR ends in shorter refueling time and lower APRR results in longer time. Refueling at optimal conditions, with as high APRR as possible require communication between vehicle and station side through an interface. Communication through the interface may not always be available due to unpredictable factors such as harsh weather or power failure. If this is the case, the fueling can still be performed with worst case assumptions on parameters, which results in utilizing a lower APRR.

2.6.2.1 SAE J2601

J2601 is an international standard protocol with minimum vehicle input for light duty hydrogen surface vehicles. The vehicle may only provide basic parameters of the onboard CHSS, that is for example total tank volume. This is when communication is possible, if not, the station side can only access tank pressure through the connection pulse [19] and assumes the worst-case scenario for the remaining factors, with or without communication.

There are two tables that decide which PRR to use, so called t_{final} tables, distributed to the station by the vehicle. Each table is based on different minimum pressure assumptions (P_{min}). The vehicle provides its initial gas pressure in the CHSS and then the station choses which t_{final} table to use depending on which P_{min} is closest in the lower bound. With information about T_{amb}, average T_{fuel} and which t_{final} table to use, a PRR is set [18]. Table I below demonstrates an example of how the t_{final}-table is designed.

TABLE I

Example of t_{final} Table

MAT T_{amb}	-40	-35	-30	-25	-20	-15	-10	-5	0
50	APRR=XY.Z	APRR=XY.Z	APRR=XY.Z	APRR=XY.Z	APRR=XY.Z	APRR=XY.Z	APRR=XY.Z	APRR=XY.Z	APRR=XY.Z
45	APRR=XY.Z	APRR=XY.Z	APRR=XY.Z	APRR=XY.Z	APRR=XY.Z	APRR=XY.Z	APRR=XY.Z	APRR=XY.Z	APRR=XY.Z
40	APRR=XY.Z	APRR=XY.Z	APRR=XY.Z	APRR=XY.Z	APRR=XY.Z	APRR=XY.Z	APRR=XY.Z	APRR=XY.Z	APRR=XY.Z
35	APRR=XY.Z	APRR=XY.Z	APRR=XY.Z	APRR=XY.Z	APRR=XY.Z	APRR=XY.Z	APRR=XY.Z	APRR=XY.Z	APRR=XY.Z
30	APRR=XY.Z	APRR=XY.Z	APRR=XY.Z	APRR=XY.Z	APRR=XY.Z	APRR=XY.Z	APRR=XY.Z	APRR=XY.Z	APRR=XY.Z
25	APRR=XY.Z	APRR=XY.Z	APRR=XY.Z	APRR=XY.Z	APRR=XY.Z	APRR=XY.Z	APRR=XY.Z	APRR=XY.Z	APRR=XY.Z
20	APRR=XY.Z	APRR=XY.Z	APRR=XY.Z	APRR=XY.Z	APRR=XY.Z	APRR=XY.Z	APRR=XY.Z	APRR=XY.Z	APRR=XY.Z
15	APRR=XY.Z	APRR=XY.Z	APRR=XY.Z	APRR=XY.Z	APRR=XY.Z	APRR=XY.Z	APRR=XY.Z	APRR=XY.Z	APRR=XY.Z
10	APRR=XY.Z	APRR=XY.Z	APRR=XY.Z	APRR=XY.Z	APRR=XY.Z	APRR=XY.Z	APRR=XY.Z	APRR=XY.Z	APRR=XY.Z
5	APRR=XY.Z	APRR=XY.Z	APRR=XY.Z	APRR=XY.Z	APRR=XY.Z	APRR=XY.Z	APRR=XY.Z	APRR=XY.Z	APRR=XY.Z
0	APRR=XY.Z	APRR=XY.Z	APRR=XY.Z	APRR=XY.Z	APRR=XY.Z	APRR=XY.Z	APRR=XY.Z	APRR=XY.Z	APRR=XY.Z
-5	APRR=XY.Z	APRR=XY.Z	APRR=XY.Z	APRR=XY.Z	APRR=XY.Z	APRR=XY.Z	APRR=XY.Z	APRR=XY.Z	APRR=XY.Z
-10	APRR=XY.Z	APRR=XY.Z	APRR=XY.Z	APRR=XY.Z	APRR=XY.Z	APRR=XY.Z	APRR=XY.Z	APRR=XY.Z	APRR=XY.Z
-15	APRR=XY.Z	APRR=XY.Z	APRR=XY.Z	APRR=XY.Z	APRR=XY.Z	APRR=XY.Z	APRR=XY.Z	APRR=XY.Z	APRR=XY.Z
-20	APRR=XY.Z	APRR=XY.Z	APRR=XY.Z	APRR=XY.Z	APRR=XY.Z	APRR=XY.Z	APRR=XY.Z	APRR=XY.Z	APRR=XY.Z
-25	APRR=XY.Z	APRR=XY.Z	APRR=XY.Z	APRR=XY.Z	APRR=XY.Z	APRR=XY.Z	APRR=XY.Z	APRR=XY.Z	APRR=XY.Z
-30	APRR=XY.Z	APRR=XY.Z	APRR=XY.Z	APRR=XY.Z	APRR=XY.Z	APRR=XY.Z	APRR=XY.Z	APRR=XY.Z	APRR=XY.Z
-35	APRR=XY.Z	APRR=XY.Z	APRR=XY.Z	APRR=XY.Z	APRR=XY.Z	APRR=XY.Z	APRR=XY.Z	APRR=XY.Z	APRR=XY.Z

The t_{final} table's top row is the mass average of fuel temperature (MAT). With an identified MAT and T_{amb} a PRR can be established. The MAT is closely related to the pre-cooling temperature but adjusted to the time it takes before target pre-cooling temperature is reached (normally max 30 seconds).

2.6.2.2 Static Data

A fueling concept that improves the refueling process by using static data from the vehicle. This includes even more data about the vehicle's CHSS than the SAE J2601 protocol. The vehicle can transmit information regarding, not only size, design, and type of tanks in the CHSS, but also thermophysical properties [18]. This protocol has two sets of t_{final} tables, identical to the SAE J2601 protocol, with different P_{min}values, further known as table A and B.

- t_{final} table A- Based on the minimum operating pressure of the vehicle's CHSS, that is P_{min}= minimum operating pressure. If $P_{\min\ \_operating} < P_{init} \leq P_{\min\ \_\text{operating}} + 5$, table A is applied
- t_{final} table B- Based on table A, with the next value being 5 MPa above the minimum operating pressure [18], ($P_{min} = P_{\min\ \_operating} + 5MPa$.) If $P_{init} > P_{min}$, table B is applied.

For example, the minimum operating pressure is 2 MPa, then table A is equal to 2 MPa and table B is set for 7 MPa. Since this protocol does not have information about the CHSS's fueling history, the protocol will assume the lower P_{min} value. For example, a vehicle may

reach a fueling station with $P_{init} = 15\ MPa$, then the static data protocol will use table B, where $P_{min} = 7MPa$. This results in a slower refueling process than if a t_{final} table derived from the correct P_{init} could have been utilized [18]. The same follows if $P_{init} = 5\ MPa$, then table A will be used.

2.6.2.3 Tgas_initial

Additional to this protocol is the data of tank temperature T_{gas_high} which is used to identify prior fueling events. A prior fueling event will cause a higher temperature than expected in the tank and thus a safety concern if fueling again. By comparing T_{gas_high} with the expected assumed worst case T_{hot_soak} (e.g. even if it is -20 °C outside the worst case expected is that the vehicle has been in soak condition in a garage at +15 °C) it is possible to avoid the overheat region and reduce the refueling time [18]. This protocol has a larger variety and less restricted P_{min} values and therefore additional and more accurate t_{final} tables. The amount of P_{min} values and the increment in between each step are pre-determined by the original equipment manufacturer (OEM) [18]. Using a more accurate t_{final} table improves the refueling process, especially at higher tank pressures. Because of the dynamic data transfer the protocol can access the initial (highest) temperature of the gas (T_{gas_high}) in each tank of the CHSS.

Similar with the static data protocol the first t_{final} table is set where $P_{min} = P_{\text{min\_operating}}$. The next tables are as described, set by the OEM (for example, $2,7,12,17,22 \dots MPa$) [18]. However, with T_{gas_high} and T_{hot_soak} in consideration it is not possible to only use P_{min} since overheat must be avoided. If $T_{gas\_high} \leq T_{hot\_soak}$ a table is chosen where P_{init} is the closest in the lower bound of the P_{min} values. As an example, a CHSS with $P_{init} = 15\ MPa$ is paired with the t_{final} table for $P_{min} = 12\ MPa$. The case where $T_{gas\_high} > T_{hot\_soak}$ the lowest P_{min} t_{final} table must be selected.

2.6.2.4 Tgas_initial+

This fueling protocol uses the tank temperature data as input prior to refueling. With additional t_{final} tables it is possible to optimize the refueling even more. The P_{min} values and intervals have the same procedure as in Tgas_initial (see section 2.6.2.3), however, when selecting a t_{final} table there is a difference. Tgas_initial+ uses multiple t_{final} tables for each P_{min} value [18].

Tgas_initial+ adds the possibility to use lower tank temperatures than worst case (T_{soak}) as starting point for the PRR calculation. It uses, $T_{soak} = T_{hot\_soak} - \Delta T$, where ΔT is a reasonable constant above zero degrees. For instance, $\Delta T = 0℃, 5°C, or\ 10℃$. With three different T_{soak} values come three t_{final} tables per P_{min} value instead of one. What table to use is regulated by comparing $T_{soak}$with T_{gas_high} using the following equation. $T_{gas\_high} < 2 * T_{soak} - T_{hot\_soak}$ [18]. If this equation is fulfilled for all T_{soak}values, then the t_{final} table with the lowest T_{soak} value is selected.

To better understand how these protocols work, see figure 7. The figure clarifies how a vehicle may choose the best suited t_{final} table for refueling.

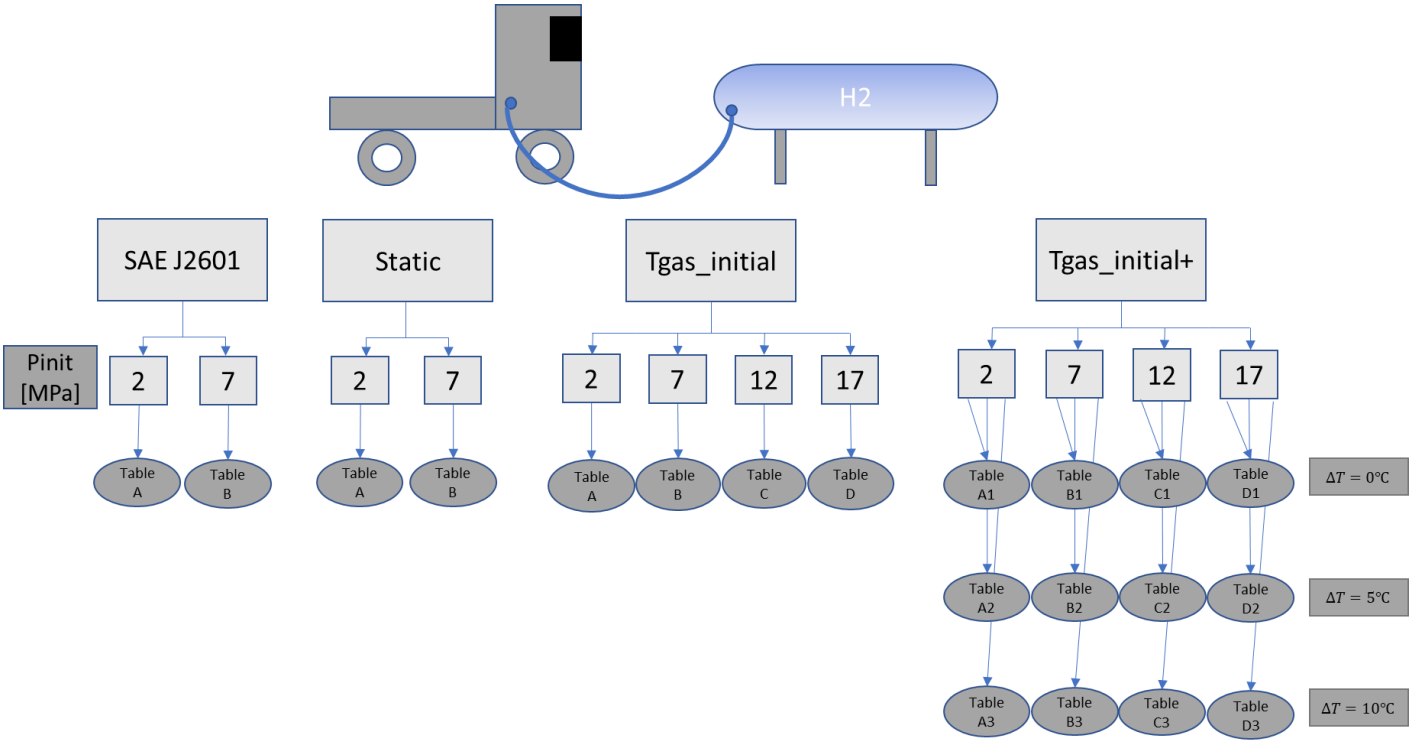

Fig 7. Fueling protocols with tfinal-tables

As described above, figure 7 is a simplified illustration of how the vehicle may choose a protocol for refueling. The different P_{min}values determine which t_{final} table to use. As demonstrated in the figure, Tgas_initial+ is the most developed of the four protocols. Which protocol is selected is dependent on how much information the vehicle may transmit.

2.7 Volvo A1 Compressed Hydrogen Storage System

The specific CHSS that is simulated is from Volvo's A1 truck. The tanks are of type IV and are horizontally aligned on top of each other placed in a steel frame. Each tank is equipped with a hand valve, also known as an "on tank valve" (OTV) that allows or restricts the hydrogen flow in and out of the tank. All tanks are connected to a multi-tank junction (MTJ) with steel pipes (type AISI 316L). Each tank consists of an inner and outer layer where the outer layer is a composite of approximately 70% T700 carbon fiber and 30% epoxy-resin and the liner is made of PA6, commonly known as nylon. Metric values of the pipes are shown in appendix A – Pipes.

3 Method

This chapter describes the different methods, including the software that is used and why they are relevant with respect to the aim of this thesis.

3.1 H2FillS

To simulate the refueling of the CHSS, a software called H2FillS, developed by the National Renewable Energy Laboratory of the U.S. Department of Energy (NREL), was used. The software is designed to simulate filling H_2 into type IV tanks and allows modeling a custom system configuration together with the complete structure or only the end (partial) of the refueling station [20]. For this project, the "H2FillS_Partial" was used since that version is focused on the area of interest for this assignment.

3.1.1 H2FillS Simulation

H2FillS is qualified to resemble a refueling process of light-duty FCEV's only [21], however, the overall components are the same as for heavy-duty vehicles. The parameters for each component are fixed with initial input values, but the user may specify the input if necessary. All parameters have an input range where H2FillS can guarantee accurate results.

H2Fills is a 1D thermodynamic model that stepwise calculates the mass and heat transfer in one dimensional section along the line of the system that is studied, in this case the fuel station to the vehicle tanks via hose, pipes, valves et cetera. The background is described in [20], however all details of the model are not available.

An example of a simulation model with a CHSS consisting of five type IV tanks is displayed in figure 8 where the individual components are configured with input values such as material density, inner volume, length, material thermal conductivity et cetera.

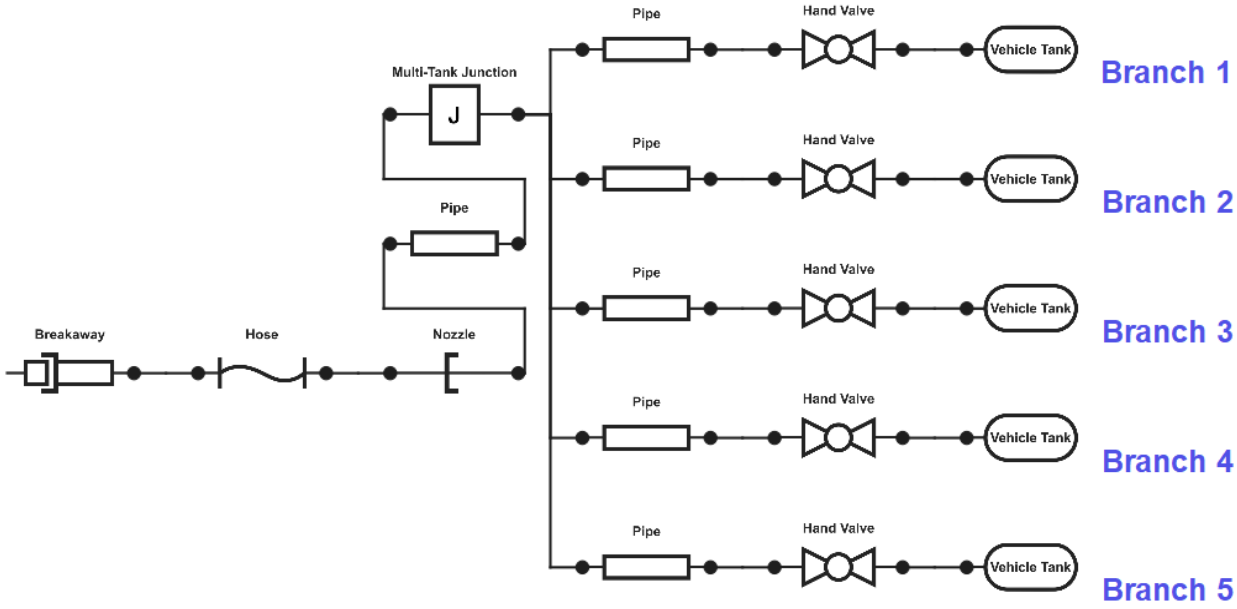

Fig. 8. Model of simulated system configuration with five identical tanks.

Since the H2FillS_Partial is used the model starts where the refueling station ends, with further components leading to a specific tank. These components are described in table II below.

TABLE II.

H2FillS Component Description

System component(s)	Description
Breakaway	The unit where H_2 leaves the refueling station
Hose	Transportation tube for H_2 to the nozzle
Nozzle	Connector from fuel station to the receptacle on the truck
Pipe(s)	Transportation for H_2 to the tanks within the CHSS
Multi-Tank Junction	5-way junction directing one inflow to five branches
Hand Valve(s) / OTV (On Tank Valve)	The unit on the tank regulating the H_2 flow in & out of tank
Vehicle Tank(s)	Main area for storage of CGH_2

The software offers several standard variations of every component including three different type IV tanks. If the user wants to specify their own components it is possible to do so. However, if the input is out of H2FillS' range, the value is displayed in a red color and may affect the results accuracy.

3.2 GT-SUITE

GT-Suite is a powerful software simulation-tool developed by Gamma Technologies, used for system & component analysis with functions ranging from mechanical, fluidal, and thermal processes among other features [22]. The results from the GT-SUITE's simulation model are used for comparison.

3.3 Granta Edu-pack

Granta Edu-Pack is a material database (student version) holding specific material data dependent on fixed tolerances through three stages. If the material is known, it is easy to access that specific material's properties such as density and thermal conductivity. This database is used to gather information about the properties of the relevant materials.

3.4 PHRYDE – D6.7

PHRYDE, described in section 2.6, released a final report (D6.7) about a three-year long study on hydrogen refueling. This report is referred to as a standard and guidance and mentions how different fueling protocols affect the refueling time depending on initial pressure and temperature in the fuel tanks. This report includes earlier results regarding the protocols, SAE J2601, Static Data, Tgas_initial and Tgas_initial+ (see section 2.6.2). The results are used as a both a guidance and comparison to this thesis's results.

4 Implementation

Before the simulations can be performed in H2FillS, the software needs to know the details of each component such as the dimensions and material of the pipes, thermal conductivity, the tanks' composite contexture and heat transfer coefficient et cetera. The data was determined from internal information or public documents found online.

4.1 Research

The simulator needs input data to execute a realistic simulation. A portion of the required data is material specific and was found on various online sources and material databases, such as Granta. Data unique for this specific configuration was gathered through Volvo's internal database and documents from subcontractors.

To store the collected data and information regarding the storage system in an accessible way, the parameters were summarized and labeled in an excel document to get a good overview of the relevant data.

4.1.1 Material properties

Common properties of H_2 and stainless steel (AISI 316L) was easily accessible from a variety of online sources and partially complemented by Granta Edu-Pack.

4.1.2 Piping

The pipe dimensions were found in internal documents. The material specific properties of the pipes were determined from online sources and Granta Edu-Pack.

4.1.3 Storage tanks

Regarding the storage tanks, partial data was provided from the supplier, Iljin, but due to the tanks' mix of carbon fiber and epoxy, some properties had to be calculated and approximated.

4.1.4 Flow coefficient

The OTVs (hand valves) on the tanks are theoretically identical. When the gas travels through the OTV the throttle process causes friction and resistance in the flow of the gas, reducing flow speed depending on the flow coefficient factor, Cv, in the valve. For the MTJ it is significantly harder to determine so the default value of 1 was used.

4.1.5 Fueling station

The data configuration from the fueling station (breakaway, hose, nozzle) comes from NREL, the simulation software developer, which is based on the SAE J2601 standard refueling protocol for light duty vehicles. This was adjusted to an estimation of what would be suitable for the purpose of fast refueling for heavy vehicles, to align with the extent of this test.

4.2 Calculations

The following part is dedicated to the calculations regarding most of the components from Fig. 8 (see section 3.1.1). Each component had to be configured prior to simulation. The input data was related to material properties, flow coefficients, pipe dimensions et cetera. However, most of the calculations were related to the storage tanks and the flow coefficient of the MTJ.

4.2.1 Storage tanks

In the simulation model there are five type IV tanks, all with the same design regarding size and material. H2FillS requires 15 input data point for each tank, shown in figure 9. All parameters must be used to run the simulation.

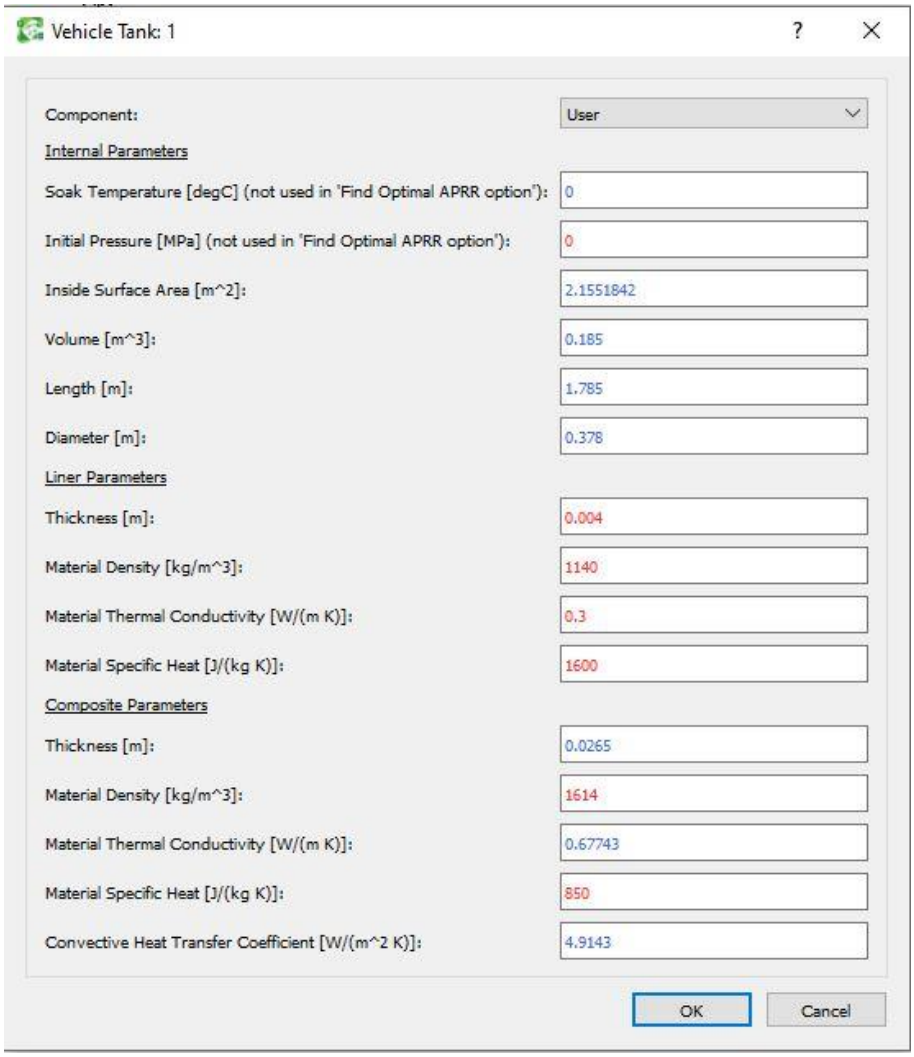

Fig. 9. Vehicle Tank Parameters.

The initial parameters indicate the entire tank where, liner parameters involve only the liner and its material, and the composite parameters are treated with respect of the CFRP as a mixture. Surface area, volume, length, thickness, and diameter regarding all three subtitles are metric values retrieved from the original CAD-model of the A1 hydrogen truck and internal data sheet from supplier. The soak temperature is often equated with the ambient temperature and the initial pressure is dependent on different scenarios when refueling. Remaining parameters are calculated and/or estimated thermodynamic properties.

4.2.1.1 Liner Parameters

There are many variations of PA6 depending on how the specific version is produced. Discussion with internal sources led to selecting properties of a cast, heat resistant version of PA6. By comparing the properties using an online material database, matweb.com, (for PA6-cast; cast, heat resistant not available), with Granta Edu-Pack the thermal properties could be identified. Matweb provided a larger range of values than Granta Edu-Pack concerning thermal properties [23]. Further discussion with internal sources supported using the intervals provided by Granta Edu-Pack. The thermal conductivity ranged between 0,294 –

0,306 $[W/mK]$ and the specific heat capacity ranged between $1570 - 1630$ $[J/kgK]$. The material's density was also provided by Granta Edu-Pack. With these ranges a value in between were selected for the simulation model.

4.2.1.2 Composite Parameters

Given from internal sources the carbon fiber is of the type T700S, however, the epoxy is not specified. Below, in table III the relevant properties of the two materials are listed.

TABLE III

Material properties CFRP.

Property/Material	Carbon Fiber T700S	Epoxy
Thermal conductivity	$9{,}6\ W/mK$	$0{,}181 - 0{,}196\ W/mK$
Specific heat capacity (cp)	$752\ J/kgK$	$1180 - 1240\ J/kgK$
Density	$1800\ kg/m^3$	$1180\ kg/m^3$

Toray Composite Materials America, Inc (Toraycma) provided the necessary data of the carbon fiber T700S [24], while Granta Edu-Pack presented the data of the epoxy. Since the epoxy was not specified, the general epoxy matrix is represented.

Thermal conductivity

Since it is a composite there must be calculations to determine the total thermal conductivity, specific heat capacity, density and lastly the convective heat transfer coefficient. The following equation presented by D.J Radcliffe and H.M Rosenberg indicates that the sum of volume per material times its conductance is equal to the total conductance along the fiber's horizontal axis [25].

$$K_{parallel} = V_{CF} * K_{CF} + (1 - V_{CF}) * K_{epoxy} \quad \textit{Eq. (1)}$$

V_{CF} is referring to the volume percentage of the carbon fiber, $K_{CF}\ and\ K_{epoxy}$ refers to the thermal conductivity of the respective material. The heat transfers vertical through the fibers of the hydrogen tanks which makes it important to consider the fiber's direction. Therefore, an empirical constant is introduced, ϵ, which is the quota of $K_{parallel}$ and $K_{vertical}$ [26]. According to D.J Radcliffe and H.M Rosenberg a reasonable ratio is $\epsilon = 10$ for composites at temperature above 10K [25]. As a result, the desired heat conductivity is:

$$K_{transverse} = \frac{K_{parallel}}{\epsilon} \quad \textit{Eq. (2)}$$

Using equation 1 and 2 to calculate the thermal conductivity of the composite transverse the fibers:

$$K_{transverse} = \frac{0{,}7*9{,}6W/mK+(1-0{,}7)*0{,}181W/mK}{10} = 0{,}67743\,\frac{W}{mK} \quad \textit{Eq. (3)}$$

Density

The total density of the composite is a mixture of the T700S and the epoxy and was calculated by using equation 4 below. The area (A) of the composite is 2,638m^2 according to the CAD-model of a single tank. The thickness (t) is read from internal documents and is 0,0265m.

$$\delta_{total,composite} = \frac{m_{total,composite}}{V_{composite}} \quad \textit{Eq.(4)}$$

$$m_{total,composite} = m_{CF} + m_{epoxy} \quad \textit{Eq. (5)}$$

$$m_{CF} = \delta_{CF} * \left(V_{composite} * 0{,}7\right) \quad \textit{Eq. (6)}$$

$$m_{epoxy} = \delta_{epoxy} * \left(V_{composite} * 0{,}3\right) \quad \textit{Eq. (7)}$$

$$V_{composite} = A * t \quad \textit{Eq. (8)}$$

The total volume, as if the composite is cut and rolled out as a square, using equation 8 is:

$$V_{composite} = 2{,}638\, m^2 * 0{,}0265m = 0{,}069907m^3 \quad \textit{Eq. (9)}$$

Calculating equation 6 and 7 separately and including them in equation 5 gives a total weight mass of 112,83 [kg]. Equation 4 gives 1614[kg/m^3] as total density of the composite.

Specific heat capacity

Calculating the specific heat capacity as a mixture of epoxy and carbon fiber is not an easy task. Therefore, an approximation is made using a formula where a mixture of two materials is treated as two separated materials, which according to [27] is theoretically possible. The formula provided states as follows:

$$C_{p,mixture} = \left(\frac{m_{CF}}{m_{total,composite}}\right) * C_{p.CF} + \left(\frac{m_{epoxy}}{m_{total,composite}}\right) * C_{p.epoxy} \quad \textit{Eq. (10)}$$

Using equation 5, 6 and 7 with the specific heat capacity for respective material gives a Cp-mixture in the range of $845{,}874 \sim 859{,}033\ J/kgK$ depending on if minimum or maximum value of the epoxy's c_p-value is used. From equation 10, a value of 850 is chosen as the input to the simulation model through discussion.

Convective heat transfer coefficient

Regarding the convective heat transfer there are some assumptions that must be done prior to the calculation. The convection is calculated from the outside layer of the composite to air Strong wind and harsh weather is not considered, which eliminates the forced convection. Only natural convection is observed.

To easier understand equation 11-13 a list of the relevant acronyms is presented below.

- h = convective heat transfer coefficient
- Nu = Nusselt number
- Pr = Prandtl number
- Ra = Rayleigh number
- g = gravitational acceleration, m/s^2
- β = 1/T for ideal gases.
- T_s = surface temperature, assumed to be same as the hydrogen in the tank, °C.
- T_{amb} = surrounding temperature of the tank, °C.
- D = diameter of the tank, m.
- v = dynamic viscosity of the air, m^2/s.

There are many different scenarios when refueling. The ambient temperature may vary extremely depending on global location and season. Since H2FillS is unavailable to accept an interval of the convective heat transfer, the input is selected as an average scenario.

The formula to calculate the convective heat transfer coefficient of a single tank, horizontally aligned, is provided by Yunus A. Çengel et al. and states as follows:

$$h = \frac{k}{D} * Nu \qquad \textit{Eq. 11}$$

where h is the convective heat transfer coefficient, k is the thermal conductivity of air at 1 atm pressure and D is the characteristic length, which in this case equals the diameter of the tank. The Nusselt number (Nu) varies with the object's shape and is without any unit [28]. Regarding a horizontal cylinder, Nu is calculated as equation 12 below.

$$Nu = \left\{ 0{,}6 + \frac{0{,}387 * Ra^{\frac{1}{6}}}{\left[1+\left(\frac{0{,}599}{Pr}\right)^{\frac{9}{16}}\right]^{\frac{4}{9}}} \right\} \qquad \textit{Eq. 12}$$

Calculating the Nusselt number requires the Rayleigh number (Ra) and the Prandtl Number (Pr). The Prandtl number is a constant depending on the air's temperature [28]), and Rayleigh's number is derived as shown in equation 13 below:

$$Ra = \frac{g*\beta*(T_s - T_{amb})*D^3}{v^2} * Pr \qquad \textit{Eq. 13}$$

With Rayleigh's number calculated, the Nusselt number was acquired and thereby the convective heat transfer coefficient. The convective heat transfer coefficient was set to 4,9143 $[W/m^2K]$, which was the average output of refueling scenarios with the ambient temperature varying between -30°C to +40°C. This result agreed with the input used in the GT-model when a truck is refueling and is only exposed to natural convection. (The value used in the GT-model is 5,0 $[W/m^2K]$).

4.2.1.3 Flow coefficient – Cv

The data and ways to calculate the flow coefficient (Cv) in imperial units for the OTV was partially provided from internal sources but complemented from online sources [29].

$$Cv = 1{,}156 * Kv \quad \textit{Eq. 14}$$

Where Kv is the flow coefficient in metric units, Since H2FillS requires the flow coefficient in imperial units. Equation 14 was used to perform the transition. In this case $Kv = 0{,}17$ [29]. Using equation 14 gives:

$$Cv = 1{,}156 * 0{,}17 = 0{,}19652 \quad \textit{Eq. 15}$$

The flow coefficient for the MTJ is initially set to 1 and remains the same since it must be evaluated in GT-SUITE to acquire a more precise flow coefficient. GT-SUITE can measure the pressure drop to in the MTJ and so access the precise flow coefficient. This type of evaluation requires more in-depth knowledge of GT-SUITE. However, using CV = 1 for the MTJ is tolerated.

4.3 Simulation procedure

The simulations were executed in a batch simulation, meaning H2FillS performed each simulation in a series, adjusting one boundary condition at a time per simulation (ambient temperature, PRR, fuel delivery temperature et cetera).

4.3.1 Test 1

In the first simulation configuration the ambient temperature and initial gas temperature in the tank were set to start with the same value and those varied between -20 °C to 35 °C, see table IV below. The PRR and fuel delivery temperature were also simulated with different values ranging from 5 to 25 MPa/min and -20 °C to 20 °C respectively. The initial tank pressure was constantly fixated at 5 MPa, or 7% SOC (kg), together with the simulation terminating condition of 97% SOC (kg). Test 1 was built as a foundation to be further developed in Test 2.

4.3.2 Test 2

The second test narrowed the parameters to fixating more values. Initial tank pressure and terminating condition remained at their constrained values but the PRR and fuel delivery temperature was set to 15 MPa/min and -20 °C respectively. The ambient and initial gas temperature in the tanks were reconfigured so initially they were not necessarily the same. This was done to simulate other scenarios such as the tanks being warmed up from standing in a garage before refueling outside in sub-zero temperatures.

4.4 Simulation process and configurations

To achieve an accurate representation of practical situations several different simulation configurations had to be considered. Some boundary conditions were fixed, and others varied to test different scenarios to see how that affected the process. A realistic variation of scenarios would be different temperatures outside due to factors such as weather, local climate and time of the year. Even the temperature inside the tanks could vary depending on driving intensity, outside temperature or if the truck recently has been parked in a garage or in the sun.

Exactly how much pressure is left in the tanks when the truck arrives at the refueling station is difficult to specify due to operators having different refueling patterns during a work cycle. In the simulations, the initial pressure is assumed to be 5 MPa, or 50 bar, when the refuel process

is initiated. That equals around 7% of the full tank capacity (70MPa, 700 bar, at 15 °C). Longer duration and higher fueling speed will increase the temperature when filling the CHSS with H_2.

4.4.1 Component configuration

Configuring and dimensioning the simulation model to fit the frame of the aim some default values had to be adjusted to more fitting values. This concerned breakaway, hose, and nozzle from the refueling station since the software is designed for light duty refueling.

4.4.2 Test 1 – Simulation boundary conditions

Test 1 is a batch of 180 tests with only two fixed conditions. Remaining conditions were set as variables. Table IV below is an overview of which condition is fixed or used as a variable.

TABLE IV

Overview and Description of Boundary

Conditions During Test 1

Fixed conditions	Value	Unit
Terminating condition: State of charge (SOC)	97	% Of max weight (37kg)
Initial tank pressure	5	MPa (50 bar)

Variable conditions	Value	Unit
Initial gas temperature in tanks	-20, -15, -10, -5, 0, 5, 10, 15, 20, 25, 30, 35	°C
Ambient temperature	-20, -15, -10, -5, 0, 5, 10, 15, 20, 25, 30, 35	°C
PRR	5, 10, 15, 20, 25	MPa/min
Fuel delivery temperature	-20, 0, 20	°C

4.4.3 Test 2 – Simulation boundary conditions

Test 2, a batch of 144 simulations that utilized only the T_{amb} and the initial gas temperature in the tank as variables. The added fixed parameters were decided with discussion internally and are presented in table V below.

TABLE V

Overview and Description of Boundary

Conditions During Test 2

Fixed conditions	Value	Unit
Terminating condition: State of charge (SOC)	97	% Of max weight (37kg)
PRR	15	MPa/min
Initial tank pressure	5	MPa (50 bar)
Fuel delivery temperature	-20	°C

Variable conditions	Value	Unit
Initial gas temperature in tanks	-20, -15, -10, -5, 0, 5, 10, 15, 20, 25, 30, 35	°C
Ambient temperature	-20, -15, -10, -5, 0, 5, 10, 15, 20, 25, 30, 35	°C

4.4.4 Simulation comparison between protocols

The protocols described in section 2.6.2 are used as guidance in this simulation batch. Two different refueling scenarios were simulated and evaluated. Each scenario utilized two different estimated initial pressures inside the tanks. This simulation batch was done to evaluate how the different protocols would apply to this thesis' boundary conditions. This is an iterative process (except for J2601, see below) where the user sets the boundary conditions and try to achieve an APRR that ends the simulation as close as possible to 97 % SOC while avoiding overheat and overpressure. In practice this was done by iteratively varying the APRR for the set input conditions in tables VI below to reach an end condition of 97% SOC, 875 bar final tank pressure and 85°C final gas temperature.

First, the APRR had to be determined, which was done using direct situations from the PHRYDE project for 5, respectively 15 MPa as initial tank pressure. These APRRs are then used on Volvo's A1 model with the same boundary conditions as in PHRYDE.

Noticeable in table VII is that the minimum operating pressure is $2MPa$. This means that the next t_{final} table will be at $2 + 5 = 7\ MPa$, which neither of the tanks will use, since their actual pressure is at $5\ MPa$. Tgas_initial+ utilizes the T_{soak} value with $\Delta T = -10$ and therefore $T_{tank} = 30°C$ instead of 40 °C.
The SAE J2601 protocol's APRR is defined by the minimum value in the given table for the fueling conditions or the value from the following equation:

$$APRR_{calculated} = 28{,}5 * \frac{v_{station}}{v_{CHSS}} \qquad \textit{Eq. 16}$$

Where $v_{station}$ is a value of volume set by the station in the range of 137-174 liters. This number was estimated to 150 liters after discussion. $v_{CHSS} = 5 * 185L = 925L$. Using equation 16 gives an APRR of 4,6 $[MPa/min]$. However, the table indicates that the actual APRR should be 3,5$[MPa/min]$. According to the standard, the lower value must be used, which is a safety precaution used for CHSS larger than 248,6 liters where the tables are not applicable. The relevant table is found in the standard. Investigating the table with 35°C ambient temperature and $5[MPa]$ as initial pressure gives an estimated target pressure that

represents 100% SOC [30]. The target pressure is 71,3 [MPa] at stated circumstances. Static and Tgas_initial has the same parameters and therefore their APRR will be equal when the iterative process is performed. The maximum APRR acquired was 6,5 $[MPa/min]$. The same was done regarding Tgas_initial+ which gave 8,5 $[MPa/min]$. These APRRs were used for a scenario provided by Volvo which is presented in table VII below.

TABLE VI

Scenario 1 case 1 Volvo, Boundary Conditions

with 5MPa as Initial Pressure

	SAE J2601	Static	Tgas_initial	Tgas_initial+
T_{amb}	35	35	35	35
T_{tank} (°C)	20	20	20	20
T_{tank_APRR} (°C)	na	40	40	30
T_{Fuel} (°C)	-20	-21	-21	-21
P_{tank} [MPa]	5	5	5	5
$P_{\text{tank\_APRR}}$ [MPa]	5	2	2	2
APRR [MPa/min]	3,5 @TP* 71,3 [MPa]	6,5	6,5	8,4

The same procedure was done with $P_{init} = 15\ [MPa]$ which gave new APRRs due to the different protocols' characteristics. This is presented below in table VII.

TABLE VII

Scenario 1 Case 2, Volvo, Boundary Conditions

with 15MPa as Initial Pressure

	SAE J2601	Static	Tgas_initial	Tgas_initial+
T_{amb} (°C)	35	35	35	35
$T_{gas(tank)}$ (°C)	20	20	20	20
T_{tank_APRR} (°C)	na	40	40	30
T_{fuel} (°C)	-20	-21	-21	-21
P_{tank} [MPa]	15	15	15	15
$P_{\text{tank\_APRR}}$ [MPa]	15	7	12	12
APRR [MPa/min]	3,5 @TP* 70,9 [MPa]	7,9	10,0	15,1

*TP = Target Pressure = 100 % SOC

Scenario 2 was developed with new conditions, which resulted in new APRRs. Scenario 2 is presented in TABLE VIII. According to the standard the APRR for SAE J2601 should be 12,9 [MPa/min] in this case while the calculated result (from equation 16) is still 4,6 [MPa/min] [30]. Following the standard, the lower APRR is used. The same iterative process was used to acquire the APRR for the remaining protocols, which are presented in table VIII below.

TABLE VIII

Scenario 2 Case 1, Volvo, Boundary Conditions

with 5MPa as Initial Tank Pressure

	SAE J2601	Static	Tgas_initial	Tgas_initial+
T_{amb} (°C)	0	0	0	0
$T_{gas(tank)}$ (°C)	0	0	0	0
T_{tank_APRR} (°C)	na	15	15	5
T_{Fuel} (°C)	-20	-21	-21	-21
P_{tank} [MPa]	5	5	5	5
$P_{\text{tank\_APRR}}$ [MPa]	5	2	2	2
APRR [MPa/min]	4,6 @TP* 66,8 [MPa]	11,7	11,7	13,9

Once again, the same procedure was done with the initial pressure at 15[MPa] and same conditions as in table IX above. The new APRRs for each protocol are presented in table IX below.

TABLE IX

Scenario 2 Case 2 Volvo, Boundary Conditions

with 15 MPa as Initial Pressure

	SAE J2601	Static	Tgas_initial	Tgas_initial+
T_{amb} (°C)	0	0	0	0
$T_{gas(tank)}$ (°C)	0	0	0	0
T_{tank_APRR} (°C)	na	15	15	5
T_{fuel} (°C)	-20	-21	-21	-21
P_{tank} [MPa]	15	15	15	15
$P_{\text{tank\_APRR}}$ [MPa]	15	7	12	12
APRR [MPa/min]	4,6 @TP* 64,9 [MPa]	16,9	30,3	40

The red values in table IX are discussed in chapter 5.2.

4.5 Case comparison between H2FillS & GT-SUITE

A batch of six simulation configurations were tested in GT-SUITE and H2FillS to compare and evaluate the reliability and accuracy of the output files from H2FillS. GT-Suite has the possibility for constructing and designing a much more complex and detailed system whereas H2FillS has a more limited configuration possibility in comparison.

These six cases are supposed to replicate different refueling scenarios. All cases utilize precooling at -20°C. The PRR is set to 15 [MPa/min] for all cases except Case 2, which uses an APRR of 5 [MPa/min]. The conditions are an out-come by evaluating test 1 and test 2 (see section 4.3.1and 4.3.2).

- Case 1: An extreme case with significant high ambient temperature and initial tank temperature.
- Case 2: An extreme case with significant high ambient temperature and initial tank temperature. Decreased PRR.
- Case 3: Winter scenario when the truck has been idle in a garage overnight.
- Case 4: Typical winter scenario with ambient temperature and initial tank temperature at 0°C.
- Case 5: A scenario of high ambient temperature combined with recent driven vehicle.
- Case 6: Winter scenario when the truck has been idle outside overnight.

Table X below clarifies all conditions set for each simulated case.

TABLE X

Overview of Boundary conditions for

Case 1-6

	Case1	Case2	Case3	Case4	Case5	Case6
Ambient temperature (°C)	35	35	-20	0	35	-20
Tank temperature (°C)	35	35	15	0	0	-20
Pressure ramp rate	15MPa/min	5MPa/min	15MPa/min			
Precooling	-20C					
Tank initial pressure	50bar					

4.6 Comparison between H2FillS & field test data

To finalize the thesis, it was of interest to check the correlation between H2FillS and reality. The goal was to configure the simulator to achieve a similar result as from the field test from the prototype predecessor, Mule 3, which has the same tanks as A1 vehicles. Figure 10 is the result from the field test with many data points to look at. However, the most interesting data is the dark blue line, which is the mass flow, the light green line, which is representing the refueling pressure (equivalent to the PRR) and the purple line, representing the average pressure.

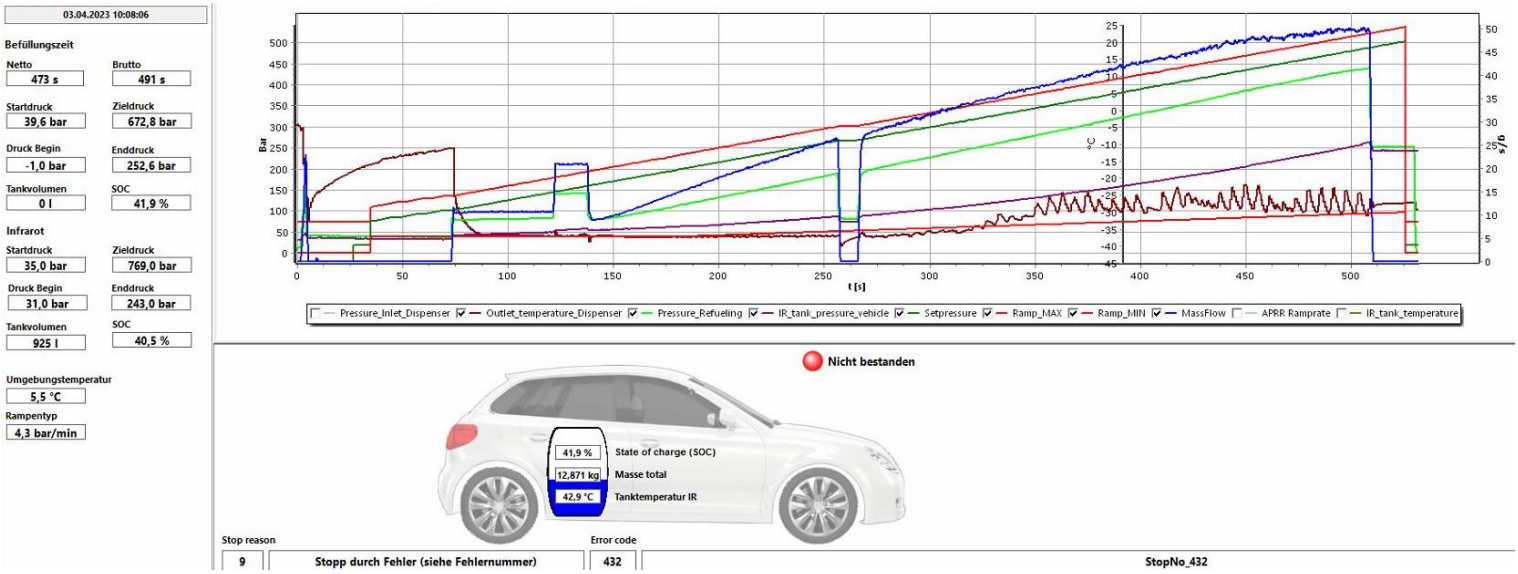

Fig. 10. Result graph from field test 1027. From [Internal documents]

The diagram presents different parameters of the refueling process over time. In this test the tanks were refueled from 31 bar to 243 bar, with a set goal of 769 bar. In practice, the fueling

stopped before end pressure was reached. The result is still valid and usable although the test failed.

By tracking the mass flow (blue line), the refueling pressure (light green line) and temperature (from the associated excel-file) a comparison could be done in H2FillS by compiling these values in a new file, which could be used as an input file in H2FillS. Some modifications were done to the input file. The first 72 seconds were omitted since there was no actual refueling during this time. The heavy mass flow drop (at approximately 250 seconds) was modified slightly to achieve a more representative APPR in the H2FillS simulation, which enabled recreating the refueling process from figure 10. The results are presented in chapter 5.4.

5 Results

The simulation resulted in a total of 180 (Test 1) + 144 (Test 2) (=324) output files with simulation data.

In figure 11 below there is an example of one refueling simulation demonstrating how the gas pressure, tank temperature and mass flow behaves during a refueling process. The y-axis represents °C for the average gas temperature, MPa for the average gas pressure and g/s for the mass flow. Time, in seconds, is displayed at the x-axis.

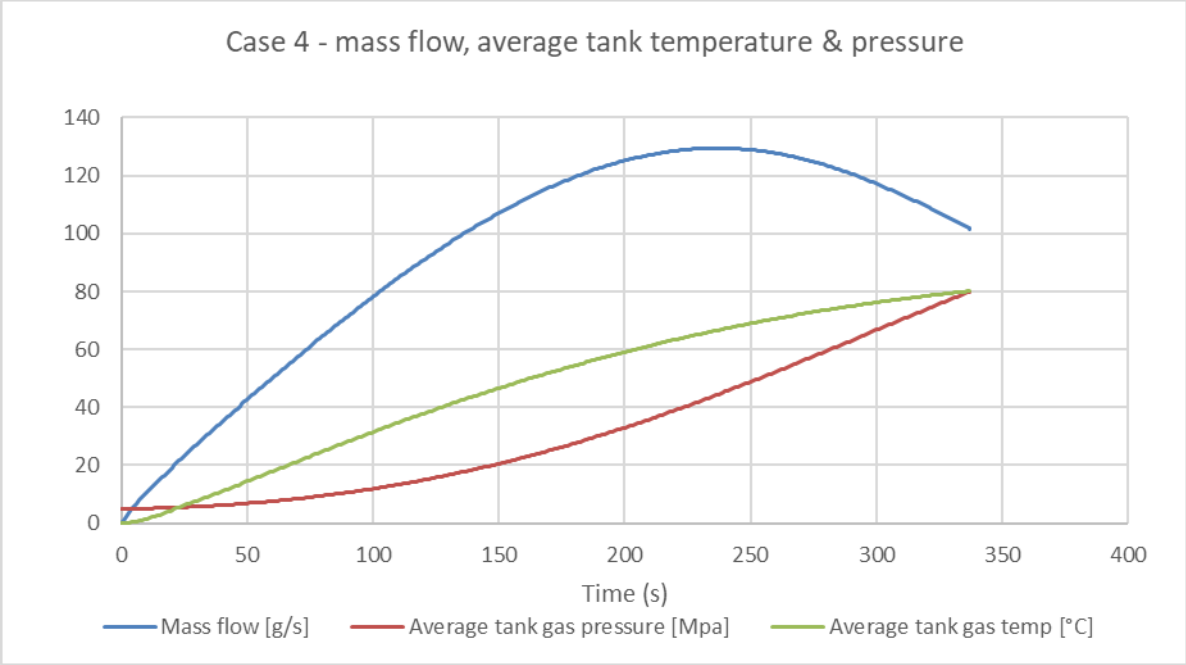

Fig. 11. Mass flow, gas pressure and tank temperature behavior during refueling

Average gas temperature follows the mass flow vaguely, but noticeable. The average pressure increases more rapidly as the mass flow increases, which is explained by figure 1 in section 2.1

5.1 Simulation results

5.1.1 Test 1

The first simulation, Test 1, resulted in a relatively broad result space that covered a set of different configurations with varied values for ambient and inner tank temperatures, pressure ramp rates and fuel delivery temperatures. Generally, the total time to refuel varied approximately between 4 to 16 minutes, the temperatures between 50 to 140°C and the pressure between 75 to 96 [MPa]. In general, the fastest fueling times (APRR 20 and 25 MPa/min) showed variation in end states between tanks which is an indication of uncertainty of the simulation accuracy for these conditions. In the worst case the SOC for one tank was only 86% for the terminating condition of 97%. However, for APRRs of 15 MPa/min and lower all tank end states were 93-97%.

This test made it clear pre-cooling is essential to meet all the set system specifications, especially regarding the gas temperature (85 °C) in the tanks. Figure 12 shows an example for

the resulting final tank temperature as a function of pre-cooling temperature. The other parameters were chosen as typical, with the ambient temperature and tank temperature at 15°C, P_{init} at 5 [MPa] and the PRR at 15 [MPa/min], and this can be seen as a generic result.

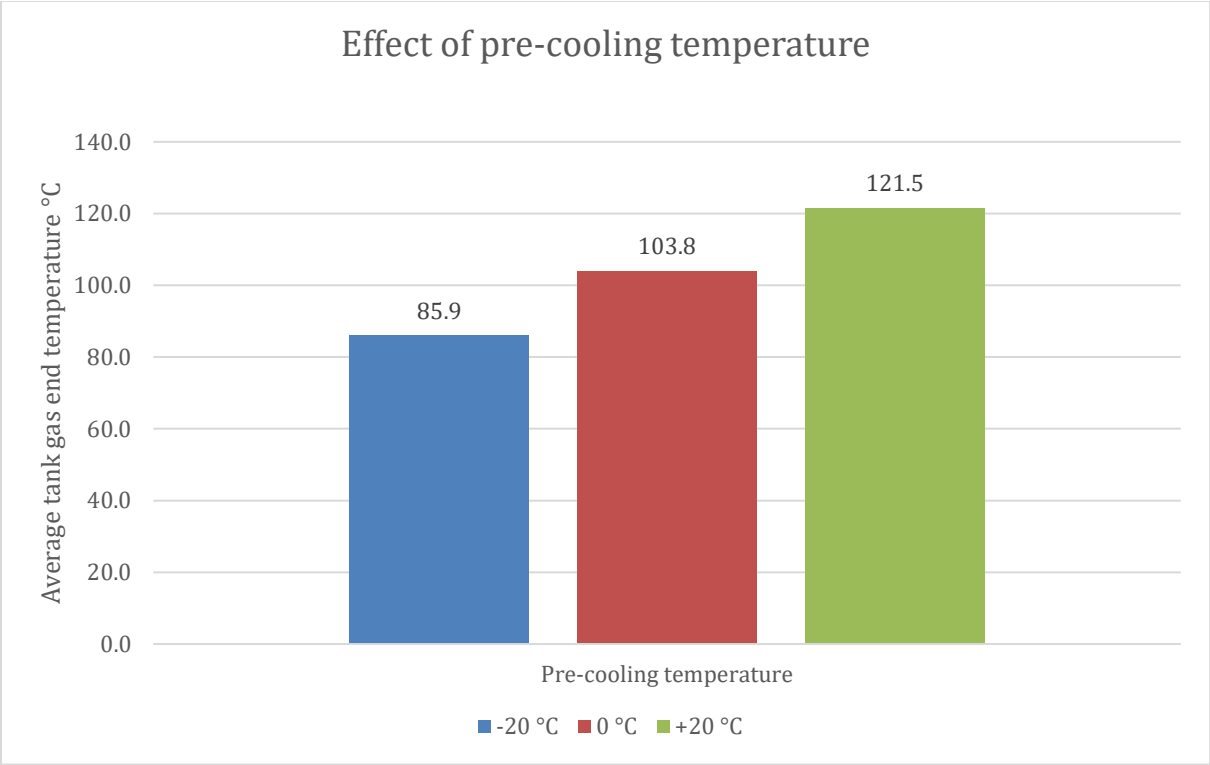

Fig. 12. Ambient & tank temperature 15 °C, initial tank pressure 5 MPa, PRR 15 MPa/min

Investigating the first results further lead to the understanding of the effects of ambient temperature. All parameters were equal to the test of the pre-cooling results above, except that the pre-cooling is fixed at -20 °C, and the ambient temperature was varied, which is displayed in figure 13.

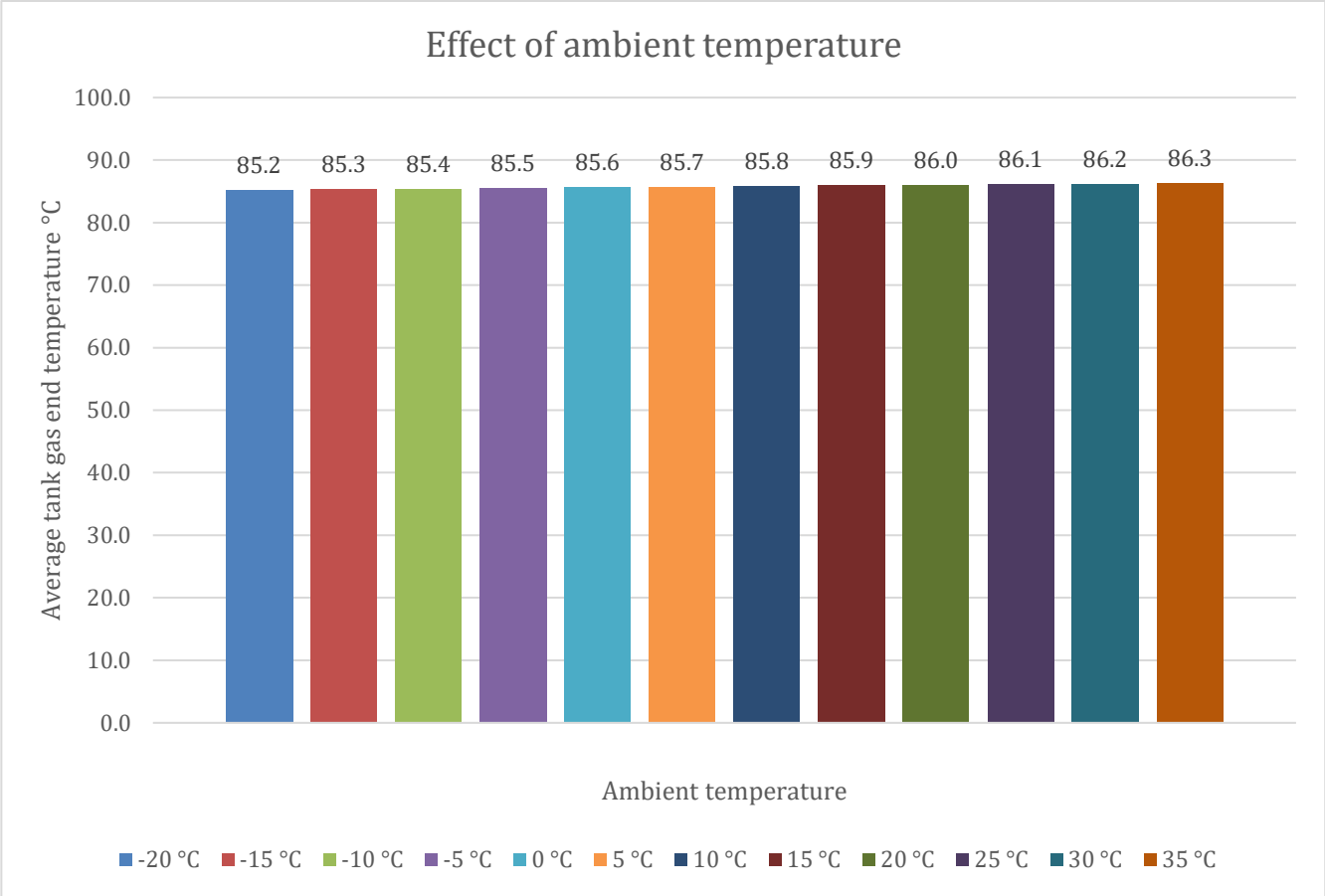

Fig. 13. Initial tank temperature 15 °C, initial tank pressure 5 MPa, PRR 15 MPa/min, pre-cool -20 °C

It is clearly shown in figure 13 that with this configuration, the ambient temperature does not play a major role in final temperature when pre-cooling is utilized. The difference between -20°C and +35°C as ambient temperature is 1,1°C.

Another observation from this test is that the gas temperature in the tanks is key for the final tank temperature at the end of the fill. The fast-fueling times allow limited amount of heat dissipation through the tank walls. This is illustrated in figure 14, where for simulation of the same typical case, with different initial tank temperatures.

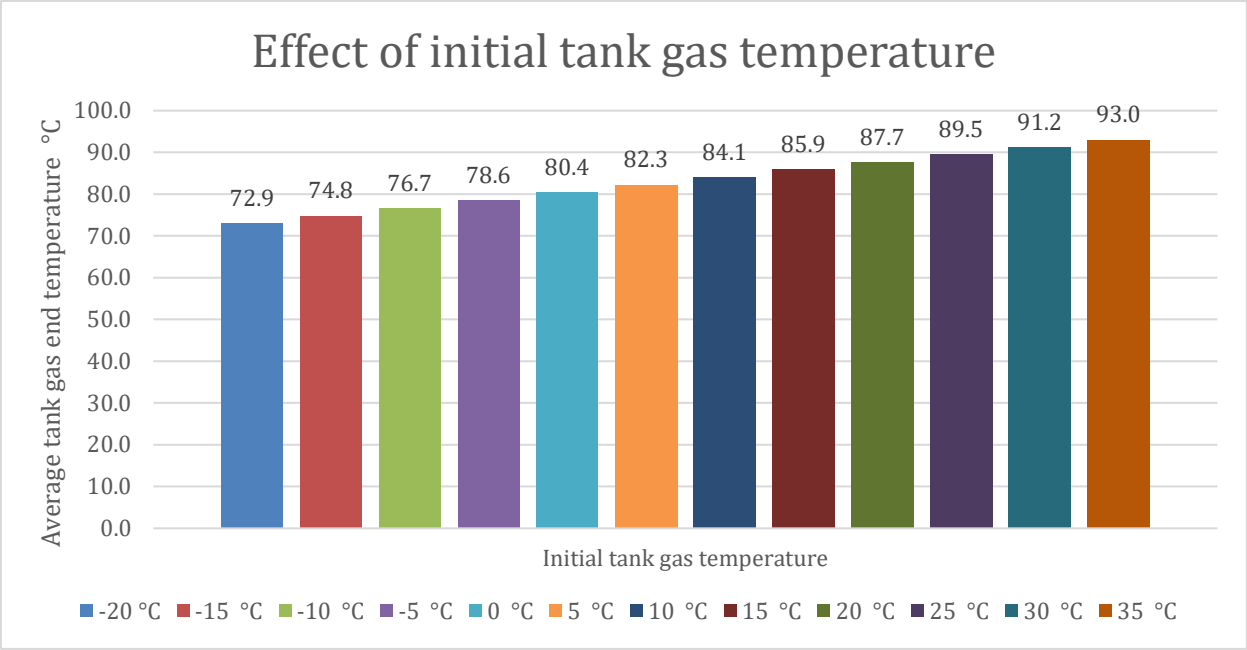

Fig. 14. Ambient temperature 15 °C, PPR 15 MPa/min, pre-cool -20 °C, initial tank pressure 5 MPa

The results from figure 12-14 above indicates that both pre-cooling and initial tank temperature must be in consideration when utilizing fast fueling for the A1 hydrogen system.

5.1.2 Test 2

After simulating Test 2, the refueling times were generally shorter, results were more aligned and showed that the ambient temperature had a minor influence on the final gas temperature in the tanks. Two simulations, one configurated with an ambient temperature of -20 °C and another of 35 °C, but otherwise identical, resulted in a final gas temperature difference of one (1) Centigrade between the two tests when one of the tanks reached 97% SOC, see table XI.

The configuration of Test 2 resulted in the refueling time ranging between 5 to 6 minutes, the temperatures between 73°C to 94 °C and the pressure between 76 to 82 bar. Table XI is a sample of the quickest and slowest refueling times for test 2. It also gives another example of initial gas temperature in the tank being a key parameter.

TABLE XI

Quickest and slowest refueling times (varied temperatures inside and outside tanks, Test 2)

Fuel Delivery Temperature [°C]	Pressure Ramp Rate [MPa/min]	Ambient Temperature [°C]	Initial Gas Temperature In Tank [°C]	Inital Tank Pressure [MPa]	Time [min] (10 min threshold)	Peak tank gas press [MPa] (87,5 MPa threshold)	Peak tank gas temp [°C] (85 °C threshold)
-20	15	-20	-20	5	5,53	80,4	73,2
-20	15	35	-20	5	5,54	80,6	74,3
-20	15	35	35	5	5,78	85,4	94,5
-20	15	-20	35	5	5,76	85,1	93,4

5.1.3 Threshold case

The configuration closest to maximum pressure and temperature, without exceeding any threshold, took 5,66 minutes and is presented in table XII.

TABLE XII

Simulation Closest to Thresholds of Pressure and Temperature Within Optimal Refueling Time

Fuel Delivery Temperature [°C]	Pressure Ramp Rate [MPa/min]	Ambient Temperature [°C]	Initial Gas Temperature In Tank [°C]	Inital Tank Pressure [MPa]	Time [min] (10 min threshold)	Peak tank gas press [MPa] (87,5 MPa threshold)	Peak tank gas temp [°C] (85 °C threshold)
-20	15	5	5	5	5,64	82,7	83,1

The result presented in table XIV above proves that it in a realistic situation is possible to reach a fair refueling time without exceeding the main limitations, pressure, and temperature, at SOC 97%. This result concerns refueling with fuel delivery temperature locked at -20 °C, PRR at 15 MPa/min with ambient and initial tank temperature being assumed as identical.

5.2 Protocol simulation results

The results of the protocol simulations are presented below in figure 15 and 16. How the APPR is defined by iteration is described in chapter 4.4.4.

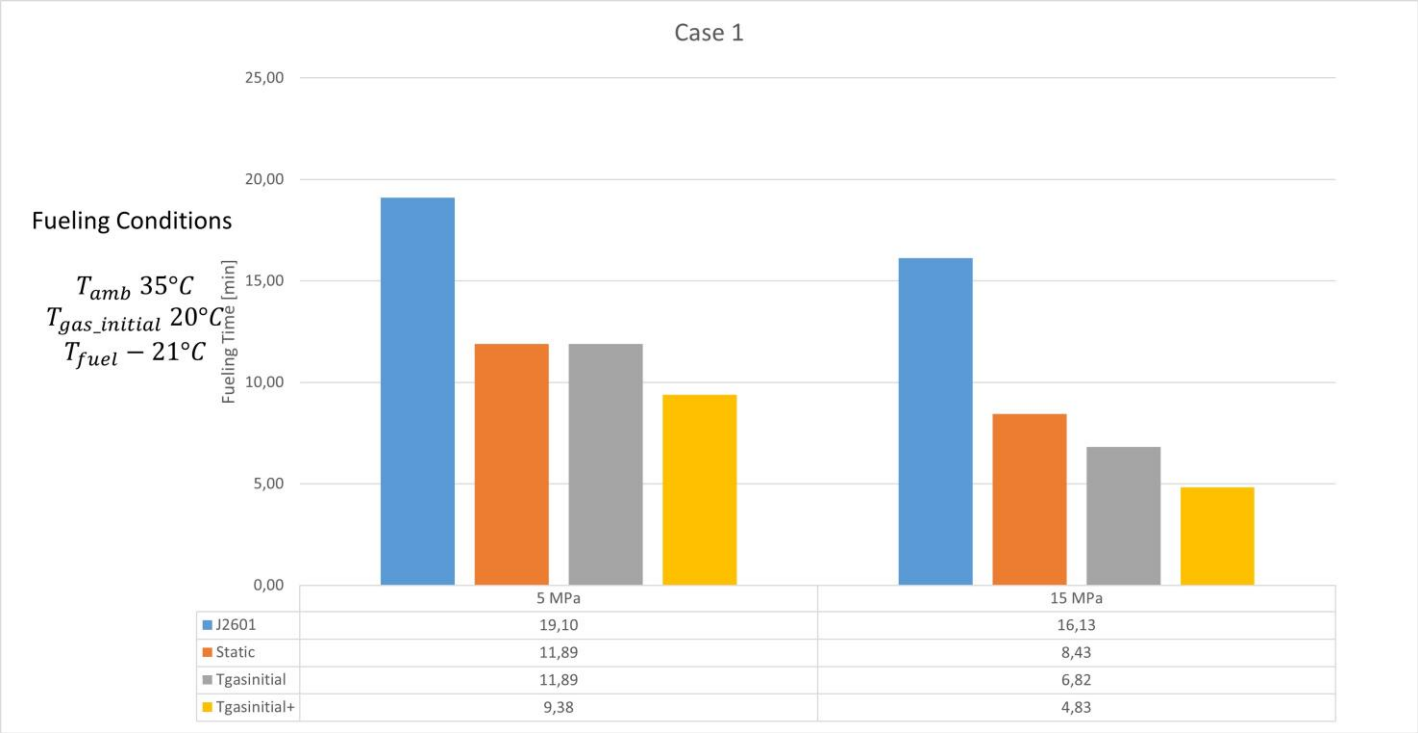

Fig. 15. Scenario 1 Case 1 and 2. Results in Minutes for Refueling with P_{init}=5/15MPa.

From figure 15 it is possible to see a decrease in refueling time depending on initial pressure, and that Tgas_initial+ is the fastest in both cases.

Noticeable from table X in section 4.4.4 (red values) is how the APRR for Tgas_initial and Tgas_initial+ were extremely high. Neither protocol exceeded the pressure or temperature limit, however sharp the APRR was. This is interpreted as unreliable results and are therefore omitted from figure 16.

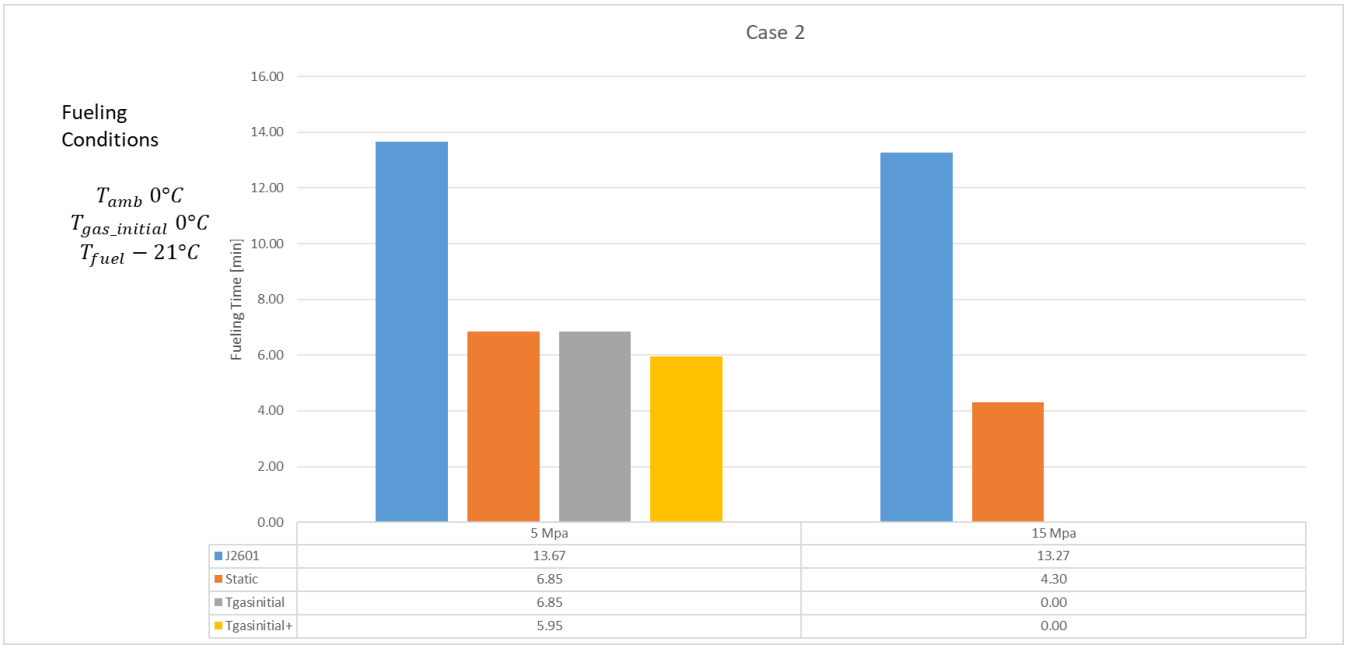

Fig. 16. Scenario 2, Case 1 and 2. Results in Minutes for Refueling with P_{init}=5/15MPa

5.3 Case comparison results between GT-Suite & H2FillS

Configuring each simulator with the appropriate values resulted in some variations in results. Each case is based on Test 2 except for Case 2 which is based on data from Test 1. The shared terminating condition in H2Fills is time. Each case has been simulated for an equal time duration to see how the other parameters and differences in methodology may influence. Selected results from the comparison between GT-SUITE and H2FillS are presented in table XIII. Effort was put into configuring the same input material parameters in GT and H2 fills for the comparison, as well as the time for when pre-cooling temperature was reached (30s).

TABLE XIII

Results From GT-SUITE Compared With

Results From H2FillS

Source of boundary conditions	Test 2	Test 1	Test 2				Simulator
	Case1	Case2	Case3	Case4	Case5	Case6	
Ambient temperature	35C	35C	-20C	0C	35C	-20C	
Tank temperature	35C	35C	15C	0C	0C	-20C	
Pressure ramp rate	15MPa/min	5MPa/min	15MPa/min				
Precooling	-20C						
Tank initial pressure	50bar						
Time (min)	5,77	15,56	5,68	5,6	5,63	5,53	H2FillS
Time (min)	5,77	15,56	5,68	5,6	5,63	5,53	GT-Suite
Final temp. (°C)	94,5	78,9	86,3	81,2	81,8	73,2	H2FillS
Final gas temp. (°C) GT	100,6	83	93,3	88,3	88,8	81	GT-Suite
Final gas pressure (MPa)	81,6	81,8	79,3	77,9	78,1	75,7	H2FillS
Final gas pressure (MPa) GT	80,3	76,5	78,5	76,8	77,4	75,3	GT-Suite

The results show a relatively good correlation between the pressure values from each simulator with Case 2 being the exception, where the result differs around 5,3 MPa. The temperature output provided by H2FillS seemed to constantly be lower compared to the output from GT-SUITE. The difference is varying between 4-8 °C.

Another comparison made was the total mass filled during refueling. The results are presented in table XIV.

TABLE XIV

Mass filled H2FillS vs GT-SUITE

	Case 1	Case 2	Case 3	Case 4	Case 5	Case 6
Tank initial mass (kg) H2Fills	3,5	3,5	3,8	4,0	4,0	4,3
Tank initial mass (kg)-GT	3,6	3,9	3,8	4,0	4,0	4,4
Total summed mass filled H2Fills	32,0	32,6	31,8	31,6	31,5	31,1
Total mass filled GT	33,8	33,8	33,8	33,6	33,7	33,6
Total mass H2FillS (initial + summed mass) (kg)	35,5	36,2	35,5	35,5	35,5	35,4
Total mass filled GT (initial+ summed mass)(kg)	37,4	37,7	37,6	37,6	37,8	38,0

According to H2FillS the total mass filled resulted between 31,1~32,6 [kg] for all cases. If the initial mass is added, the total mass equal approximately 35~36 [kg]. GT-SUITE tends to fill more hydrogen into the tanks.

5.4 Results and validation of field test data with H2FillS

The data regarding hose (breakaway) pressure from the field test (section 4.6) was input to H2FillS and yielded output data similar to the results from the field test.

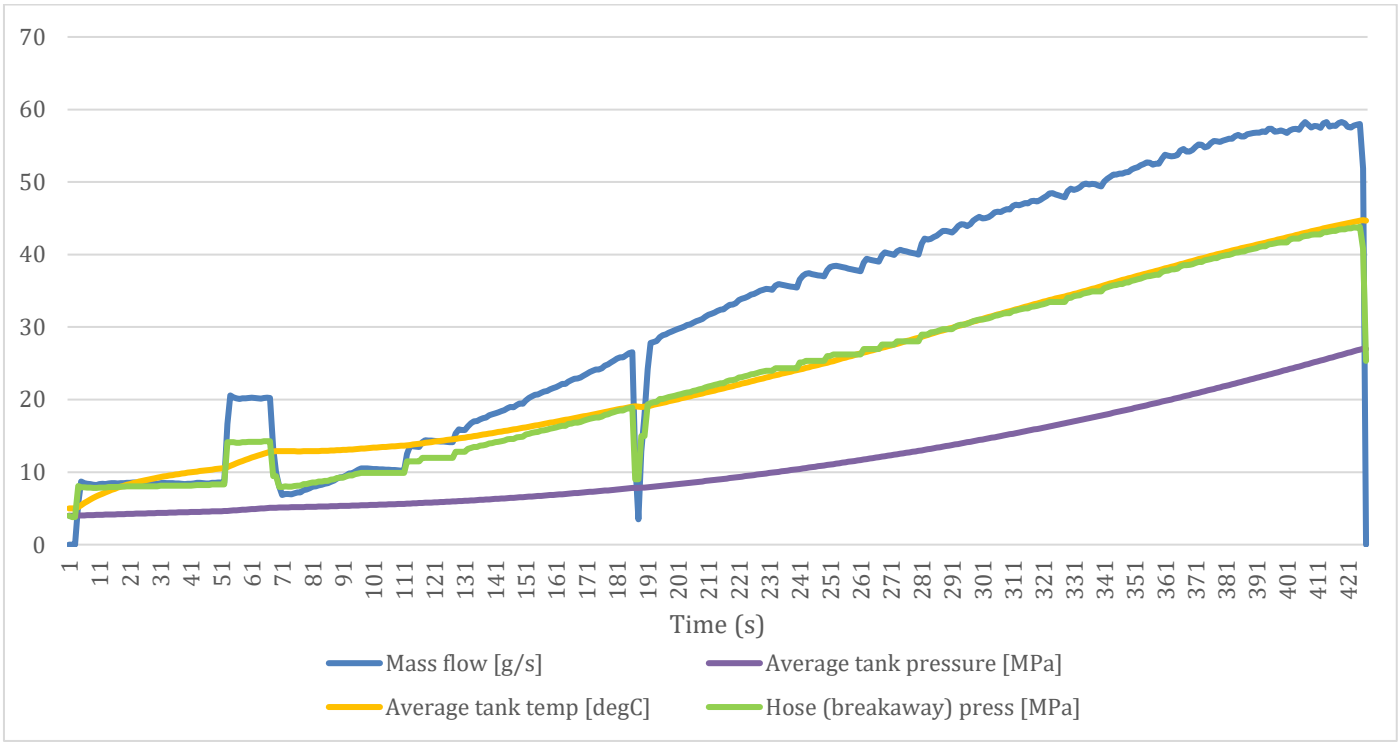

Fig. 17 H2FillS validation graph with field test input

Table XV presents the results from the comparison. H2FillS overshoots mass flow, average gas end temperature & pressure and total mass filled.

TABLE XV

Validation data

Parameter	H2FillS simulation	Field test	Difference
End mass flow	57 g/s	50 g/s	7 g/s
Average gas end pressure	27 MPa (270 bar)	26 MPa (260 bar)	1 MPa (10 bar)
Average gas end temperature	44,7 °C	43,9 °C	0,8 °C
Total mass filled	13,3 kg	12,9 kg	0,4 kg

5.5 Assessment of system pressures and temperatures from dispenser to tank outer surface

The output data in H2 fills gives the possibility to follow the physical conditions from dispenser to the vehicle. This can give some further insights on pressure drops and temperature gradients, which for example can give input to design of the fuel system. For the six cases described in section 4.5 we have investigated the pressures and temperatures given. This is illustrated in figure 17 and 18 with results shown in table XVI and XVII.
The station provides a pressure higher than what is the pressure in the downstream components, due to restrictions in the flow. This is illustrated in figure 17 with associated results in table XVI.

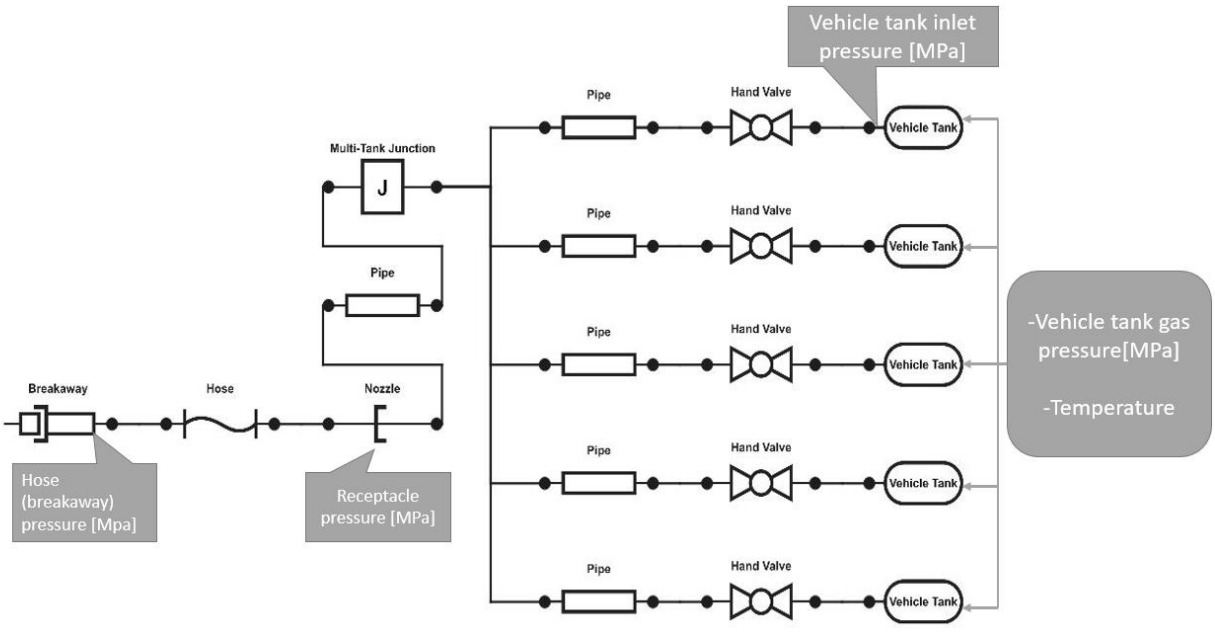

Fig. 18. Pressure in system.

TABLE XVI

Final pressure at different components

Pressure; Case	Pressure Ramp Rate [MPa/min]	Hose (breakaway) press [MPa]	Receptacle press [MPa]	Vehicle tank inlet press [MPa]	Vehicle tank gas press [MPa]
1	15	91.6	89.8	83.6	82.6
2	5	82.8	82.5	81.9	81.8
3	15	90.1	88.2	81.5	80.4
4	15	89.3	87.3	80.3	79.0
5	15	89.4	87.4	80.4	79.2
6	15	87.9	85.8	78.3	76.9

As can be seen the total pressure drop is approximately 10 [MPa], except for case 2, which can be explained by the lower PRR

Temperature gradients will occur in the system from cold delivered hydrogen from the dispenser to hot hydrogen in the tank and the heat dissipation through the tank walls. Faster heat dissipation is a benefit for the fueling as this has a cooling effect on the tank gas temperature. However, as can be seen for the quite short fueling times in cases 1,3-6 there is quite a small change in outer surface temperature of the tank. However, for case 2 with longer fueling time the change in outer surface temperature is significant. This is a nice illustration of how longer fueling times allow for more heat dissipation and lower end gas temperatures in the tanks. Figure 19 is a simplified overview of a single tank's heat measure-points from H2FillS.

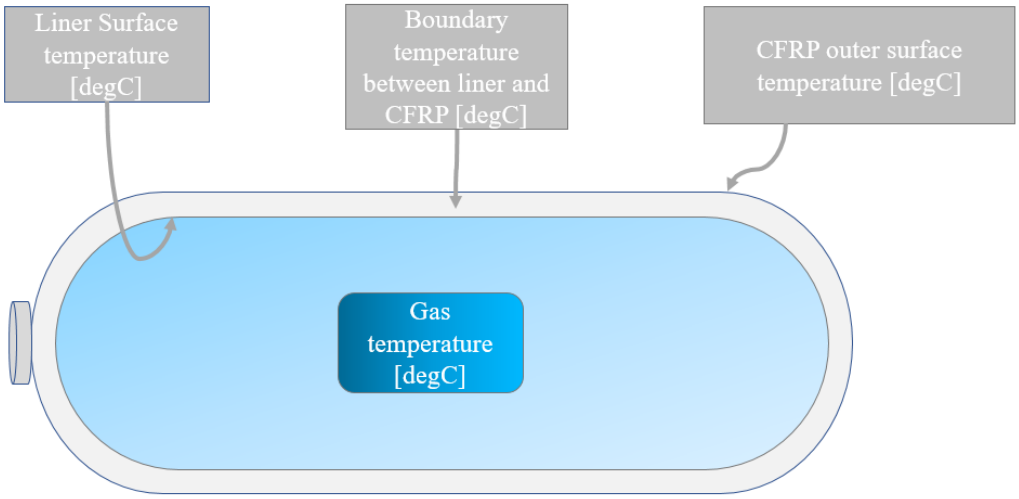

Fig. 19. Temperature measurement points in tank.

TABLE XVII

Final temperatures of a tank

Temperature; Case	Pressure Ramp Rate [MPa/min]	Initial Gas Temperature In Tank [degC]	Ambient Temperature [degC]	Vehicle tank gas temp [degC]	Vehicle tank liner surface temp [degC]	Vehicle tank boundary temp between liner and CFRP [degC]	Vehicle tank CFRP outer surface temp [degC]
1	15	35	35	93.9	91.9	64.2	37.1
2	5	35	35	78.8	77.6	65.2	46.9
3	15	15	-20	85.6	83.3	49.6	13.8
4	15	0	0	80.6	78.0	40.0	2.7
5	15	0	35	81.2	78.7	40.8	6.3
6	15	-20	-20	72.6	69.8	25.7	-17.1

Table XVII shows that the PRR is highly related to the final pressure since case 1 and case 2 were simulated with the same boundary conditions except their PRR, but the temperature is different at almost every measure point. Noticeable is that for case 2, the surface temperature is higher than case 1. Case 2 took 10 more minutes to refuel than case 1, which means that the tanks were exposed to the heat transfer for a longer period. There are no results of case 1 after disconnected from the station. For example, if the truck is stationary for 10 minutes after the refueling there is a possibility that case 1 will reach the same surface temperature as in case 2 due to the heat dissipation from the gas inside the tank. However, this is not confirmed.

6 Discussion

As of today, the software H2FillS, that the data in this report relies on, is not yet developed to be used for heavy duty vehicle tank refueling at the flow rate being simulated. It is possible to enter custom values for a set of parameters but only within a certain interval can the developer (NREL) guarantee the precision of the output. During the configuration of the H2FillS model some values were set outside the interval. The simulations may still be accurate and reliable; however, it is potentially a source of error. Some variations in data between tanks, especially for higher APRR is an indication that these results should be assumed to be of less accuracy.

Calculations for the convective heat transfer coefficient, material specific heat conductivity and material specific heat for the composite mix had to be calculated based on the known material composition. Measurement data from supplier would have been preferable but was not available.

Also, when batch simulating for Test 1 some data was simulated outside of H2FillS's recommended interval. The accepted pressure ramp rate interval ranges from 15 to 25 MPa/min, although we see that especially for APRRs above 20 MPa/min the results are inconsistent. Also, the breakaway, hose and nozzle were configurated outside the specified interval which could affect the results.

The simulations reveled that the ambient temperature did not affect the refueling process as presumed regarding the final temperature inside the tank. The biggest influence had the initial tank temperature and the temperature of the delivered fuel.

The total mass hydrogen injected in the tanks is as important as keeping the refueling within the limits of pressure, temperature and refueling time. All simulations started with the tanks initial pressure at 50 bar, which approximately is 3,5~4,2 kg in total for all tanks depending on temperature. The aim was to reach 37 kg when fully refueled and H2FillS was relatively accurate with the results when compared to the GT-SUITE model. In the simulations from H2FillS the different tanks reached different SOC when finished, with that, it seems the difference in lengths of the input pipes has an impact on the distribution of H_2 between the tanks.

It is suggested to perform further validations as a next step, the comparison between H2FillS and the field test was only one single test and should be evaluated further. Although there are some differences in the prototypes Mule 3 and A1 it should be possible to perform a validation. The data in the simulations are based on system dimensions and piping from A1 while the data from the field test comes from Mule 3. The tanks are identical and although the piping should not differ too much, they are not identical.

During this thesis there have been some concerns regarding H2FillS accuracy. H2FillS uses fixed parameters with ranged intervals. Some of input data used in this thesis were outside these intervals, which according to NREL would mean that the results could not be guaranteed to be accurate. Quick sensitivity analyses were done in the initial stages of the work, and it was seen within the material parameters and other input data selected there was relatively small impact on the final result. An exception is for very high PRR where the model results were fluctuating between simulations and thus seen as unreliable. Analyzing the simulation model further H2FillS has some restricted design possibility of the components

designed by the user. As an example, the geometry and bends of the pipes and coefficient intervals. The software is also does not take important factors, such as leak checks, in consideration, but this likely has only a small influence. Inconclusion, further validation work is necessary, by valuable learnings have been reached in what parameters that influence the fueling time the most and how to implement fueling protocols. Also, relative comparison between different cases seems to be possible.

Some of the results are as described, compared with GT-SUITE. This is because of how GT-SUITE has more in-depth configuration possibility and more detailed flow parameter monitoring. It is possible to track other influencing factors such as leaks and heat development in certain points inside the tanks.

During the comparisons between GT-SUITE and H2FillS it has been one parameter standing out. H2Fills constantly presents a lower temperature value than GT-SUITE. If the GT-SUITE-model is as accurate as alleged, it is another indication that H2FillS is not yet reliable for larger CHSSs. A constant delivery of lower temperature values is a major safety deficiency. For those reasons, a simulator like H2FillS should be more conservative, especially considering the simplicity of the model. However, in the comparison the simulator tended to overshoot the results slightly, which could be considered a conservative approach, for safety reasons. More work and field data are however needed to completely validate both GT and H2Fills results. A discussion with NREL on this topic is suggested as a next step.

7 Conclusion

In this chapter, conclusions from the results are drawn and the aim of the report is discussed. The goal was to be able to refuel the tanks on a Volvo's hydrogen truck 'A1' at around 10 minutes without exceeding a pressure of 87,5 MPa, or a temperature of 85 °C or fill more than 100% SOC.

The thesis found that it through simulations is possible to perform refueling in max 10 minutes without compromising the boundary conditions. A practical solution requires the H_2 to be pre-cooled to at least -20 °C when leaving the tank station to not exceed temperature thresholds. Newly developed protocols for fueling of larger heavy duty tank systems are also necessary to achieve the target.

One of the goals was to fill a total of ~37 [kg] H_2 in the system. H2FillS seemed to be quite accurate of this parameter and the total simulated mass were 35~36 [kg] while avoiding overpressure and overheat, which is fully acceptable. However, this is highly dependent on the initial tank temperature

H2FillS is an easy tool to use but require further development if simulation on trucks shall be accurate and reliable. Since the software has shown not to be as conservative as it should have been it would not be recommended to rely on the output provided by the simulations until further validation work is done.

Regarding using H_2 as energy carrier, no solution is without deficiencies. H_2 can be used in more ways than to power a FC but using H_2 has challenges to overcome as well as the potential to be used as fuel in a new generation of propulsion systems. No matter the final use, refueling simulation is relevant for research and development purposes which could help speed up the transition progress towards fossil-free transportation. This thesis has provided some insights to the application of fueling protocols, but more validation work is needed, as well as investigations of pros and cons with the different fueling approaches.

8 References

[1] WRI; ClimateWatch, ”Distribution of greenhouse gas emissions worldwide in 2019, by sector,” Statista, 28 July 2019. [Online]. Available: https://www-statista-com.eu1.proxy.openathens.net/statistics/241756/proportion-of-energy-in-global-greenhouse-gas-emissions/?locale=en. [Använd 29 03 2023].

[2] J. Thangavelautham, Degradation in PEM Fuel Cells and Mitigation Strategies Using System Design and Control, T. Taner, Red., Tucson, Arizona: InTechOpen, 2017, p. 212.

[3] G. R. F. B. P. E. Željko Penga, ”Degradation Mechanisms in Automotive Fuel Cell Systems,” European Commision, 2017.

[4] A. Buis, "The Atmosphere: Getting a Handle on Carbon Dioxide," *Global Climate Change: Vital Signs of the Planet*, 9 October 2019.

[5] M. M. R. H. S. Röck, "JEC Tank-To-Wheels report v5:," Publications Office of the European Union, Luxembourg, 2020.

[6] College of the Desert, ”Hydrogen Properties,” California, 2001.

[7] D. O. K. Dr. Klaas Kunze, *Cryo-compressed hydrogen storage*, Oxford: BMW Group, 2012, p. 33.

[8] R. Caponi, A. Monforti Ferrario, E. Bocci, G. Valenti och M. Della Pietra, ”Thermodynamic modeling of hydrogen refueling for heavy-duty fuel cell buses and comparison with aggregated real data,” *International Journal of Hydrogen Energy*, vol. 46, nr 35, pp. 18630-18643, 2021.

[9] Britannica, ”Joule–Thomson effect,” 06 Mars 2023.

[10] toppr, "Joule Thomson Effect," toppr, 2023.

[11] H. W. Langmi, N. Engelbrecht, P. M. Modisha and D. Bessarabov, "Chapter 13-Hydrogen storage," in *Electromechanical Power Sources: Fundamentals, System, and Applications (Hydrogen productions by water Electrolysis)*, 2021, p. 456.

[12] H. Barthélémy, ”Hydrogen storage - Industrial prospectives,” Elsevier Ltd, Paris, 2012.

[13] Regents of the University of California, "Modeling the Fuel Cell Reaction," 2011.

[14] Department of Energy, "Fuel Cells".

[15] Umicore, "Fuel cells vs. batteries: what’s the difference?," Umicore, 2022.

[16] D. C. Garcia-Navarro, ”What does a hydrogen refueling station look like?,” 05 06 2021. [Online]. Available: https://hydrogen-central.com/what-hydrogen-refueling-station-look-like/. [Använd 13 04 2023].

[17] ludwig bölkow systemtechnik, "PHRYDE-Protocol for Heavy-Duuty Hydrogen Refuellig," ludwig bölkow systemtechnik GmbH (LBST), 2020. [Online]. Available: https://lbst.de/prhyde/. [Accessed 05 04 2023].

[18] N. Hart, C. Due Sinding, S. Mathison, S. Quong, V. Mattelaer, A. Ruiz, A. Grab (Nikola), A. Kvasnicka, C. Spitta, F. Ammouri, E. Vyazmina, V. Ren, G. Lodier, Q. Nouvelot, T. Guewouo, J. Martin, D. Crouslé, N. Benvenuti, C. Kutz and M. Zerta, "Deliverable D6.7 PHRYDE Results as Input for Standardisation," ludwig bölkow systemtechnik, Ottobrunn/Munich, 2023.

[19] W. James, J. Schneider and S. Mathison, "An Introduction to SAE Hydrogen Fueling Standardization," 11 09 2014. [Online]. Available:

https://www.energy.gov/sites/prod/files/2014/09/f18/fcto_webinarslides_intro_sae_h2_fueling_standardization_091114.pdf. [Accessed 12 04 2023].

[20] T. Kuroki, K. Nagasawa, M. Peters, D. Leighton, J. Kurtz, J. Sakoda, M. Monde och Y. Takata, ”Thermodynamic Modeling of Hydrogen Fueling Process from High Pressure Storage Tanks to Vehicle Tank,” Energy Conversion and Storage Systems Center, National Renewable Energy Laboratory, Colorado, 2021.

[21] NREL.gov, "H2FillS: Hydrogen Filling Simulation," [Online]. Available: https://www.nrel.gov/hydrogen/h2fills.html. [Accessed 02 05 2023].

[22] Gamma Technologies, "WHAT IS GT-SUITE?," Gamma Technologies, Westmont.

[23] MatWeb, ”Overview of materials for Nylon 6, Cast,” NA. [Online]. Available: https://matweb.com/search/DataSheet.aspx?MatGUID=8d78f3cfcb6f49d595896ce6ce6a2ef1. [Använd 05 03 2023].

[24] Toray Composite Materials America, Inc., ”T700S STANDARD MODULUS CARBON FIBER,” Toraycma, Decatur, Alabama, 2018.

[25] D. Radcliffe och H. Rosenberg, ”The thermal conductivity of glass-fibre and carbon-fibre/epoxy composites from 2 to 80 k,” *Cryogentics,* vol. 22, nr 5, pp. 245-249, 1982.

[26] C. He och J. Xu, ”Finite Element Analysis of the Thermal Conductivity and the Specific Heat of Carbon Fiber Reinforced Plastic (CFRP) Composites,” i *2020 International Conference on Artificial Intelligence and Electromechanical Automation (AIEA)*, Tianjin, China, 2020.

[27] Thermtest instruments, ”Rule of Mixtures Calculator for Heat Capacity,” Thermtest instruments, 30 01 2019. [Online]. Available: https://thermtest.com/thermal-resources/rule-of-mixtures. [Använd 13 03 2023].

[28] Y. A. Çengel, J. Cimbala och R. H. Turner, ”Natural Convection,” i *Fundamentals of Thermal-Fluid Sciences*, vol. 5, New York, McGraw-Hill Education, 2017, pp. 830-833.

[29] R. J. M. Rao, ”Control Valve Relation between Cv and Kv,” Inst Tools.

[30] SAE International, "Fueling Protocols for Light Duty Gaseous Hydrogen Surface Vehicles J2601_202005," SAE International, United States, 2020.

[31] Internal Energy Agency, "CO2 Emissions," Internal Energy Agency, Paris, 2023.

Appendix A – H2FillS simulation model data input

Storage tanks

	Internal Parameters					
Storage tanks	**Soak temperature** [°C]	**Initial Pressure** [MPa]	**Inside Surface Area** [m^2]	**Volume** [m^3]	**Length** [m]	**Diameter (inner)** [m]
Storage tanks 1-5 (Input values)	Variable	Variable	2.1551842	0.185	1.785	0.378
Default value	23	2	1.1	0.099	0.855	0.42
H2FillS - Guaranteed accuracy value interval	0-35	2-5	0.3-2.2	0.01-0.249	-	0.183-0.513

	Liner Parameters			
Storage tanks	**Thickness** [mm]	**Material Density** [kg/m^3]	**Material Thermal Conductivity** [W/(m K)]	**Material Specific Heat** [J/(kg K)]
Storage tanks 1-5 (Input values)	4	1140	0.3	1600
Default value	5	945	0.5	2100
H2FillS - Guaranteed accuracy value interval	0.005-0.00546	945-946	0.5-0.52	2100
Material data interval			0.294-0.306	1570-1630

	Composite Parameters				
Storage tanks	**Thickness** [mm]	**Material Density** [kg/m^3]	**Material Thermal Conductivity** [W/(m K)]	**Material Specific Heat** [J/(kg K)]	**Convective Heat Transfer Coefficient** [$W/(m^2 K)$]
Storage tanks 1-5 (Input values)	26.5	1614	0.67743	850	4,9143
Default value	31.6	1494	0.5	1120	8

H2FillS - Guaranteed accuracy value interval	22.2-38.3	1494-1580	0.5-0.75	1120-1300	4.5-20
Material data interval			6.7743	845.874-859.033	

Breakaway:

Breakaway	**Flow coefficient** [Cv]	**Inside diameter** [m]	**Outside diameter** [m]	**Length** [m]	**Material Density** [kg/m^3]	**Material Thermal Conductivity** [W/(m K)]	**Material Specific Heat** [J/(kg K)]	**Convective Heat Transfer Coefficient** [W/(m^2 K)]
Value	2	0.008	0.04	0.56	7900	5	659	10
Default values	1	0.004	0.025	0.56	7900	5	659	10
H2FillS - Guaranteed accuracy value interval	1	0.004-0.00516	0.017-0.025	0.5-0.56	7900-8000	1.5-16.7	500-700	0.1-20

Hose:

Hose	**Hose Length** [m]	**Inside diameter** [m]	**Outside Diameter** [m]	**Material Density** [kg/m^3]	**Material Thermal Conductivity** [W/(m K)]	**Material Specific Heat** [J/(kg K)]	**Convective Heat Transfer Coefficient** [W/(m^2 K)]
Value	3.5	0.01	0.02	3694	1.5	558	10
Default values	3.5	0.00516	0.012	3694	1.5	558	10
H2FillS - Guaranteed accuracy value interval	3.5-5	0.00516-0.0063	0.012-0.013	3694	1.5	558	0.1-20

Nozzle:

Nozzle	**Flow coefficient** [Cv]	**Inside diameter** [m]	**Outside Diameter** [m]	**Length** [m]	**Material Density** [kg/m^3]	**Material Thermal Conductivity** [W/(m K)]	**Material Specific Heat** [J/(kg K)]	**Convective Heat Transfer Coefficient** [W/(m^2 K)]
Value	2	0.008	0.04	0.36	7900	5	659	10
Default values	1	0.004	0.0275	0.36	7900	5	659	10
H2FillS - Guaranteed accuracy value interval	1	0.004-0.00516	0.0017-0.00275	0.36-0.5	7900-8000	1.5-16.7	500-700	0.1-20

MTJ:

MTJ	**Flow coefficient** [Cv]
Value	1
Default value	1
H2FillS - Guaranteed accuracy value interval	0.75-1.3

Hand valves:

Hand Valves	**Flow coefficient** [Cv]
Hand Valve 1	0,19652
Hand Valve 2	0,19652
Hand Valve 3	0,19652
Hand Valve 4	0,19652
Hand Valve 5	0,19652
Default value	1
H2FillS - Guaranteed accuracy value interval	0.75-1.3

Pipes:

Pipes	**Inside diameter** [mm]	**Outside Diameter** [mm]	**Pipe Length** [mm]	**90-deg. Bends** [amount]	**Material Density** [kg/m^3]	**Material Thermal Conductivity** [W/(m K)]	**Material Specific Heat** [J/(kg °C)]	**Convective Heat Transfer Coefficient** [W/(m^2 K)]	**Pipe Thickness** [mm]
To tank 1	3.05	6.35	1066.137	1	7900	16.5	500	5	1.65
To tank 2	3.05	6.35	1149.203	3	7900	16.5	500	5	1.65
To tank 3	3.05	6.35	582.9716	3	7900	16.5	500	5	1.65
Pipe to tank 4	3.05	6.35	603.8808	3	7900	16.5	500	5	1.65
Pipe to tank 5	3.05	6.35	1227.402	4 (3)*	7900	16.5	500	5	1.65
MTJ input pipe	6.2	12	526.6798	1	7900	16.5	500	5	2.9
Default value	0.00516	0.00956	3	0	8000	16.3	500	5	
H2FillS - Guaranteed accuracy value interval	2.27-11.13	6.35-19.05	250-50000	No limit	7900-8000	16.3-16.7	500-700	0.1-20	
Material data intervals (T=23°C)	-	-	-	-	7870-8070	13-17 (14.2)	490-530 (486)	25.32	

*Extra bends along the pipe. Therefore +1 bend is added.